Assessing Above Ground Biomass C-storage in Bamboo (Belgium)

Auteur : Bernard, Guillaume
Promoteur(s) : De Mil, Tom
Faculté : Gembloux Agro-Bio Tech (GxABT)
Diplôme : Master en bioingénieur : sciences et technologies de l'environnement, à finalité spécialisée
Année académique : 2022-2023
URI/URL : http://hdl.handle.net/2268.2/18158

Assessing Above Ground Biomass C-storage in Bamboo (Belgium)

Guillaume BERNARD

THESIS PRESENTED FOR THE OBTAINING OF A DEGREE IN
BIOENGINEERING IN ENVIRONMENTAL SCIENCES AND TECHNOLOGIES

ACADEMIC YEAR 2022 - 2023

CO-PROMOTERS: Pr. Jeroen MEERSMANS, Pr. Tom DE MIL

LIÈGE université
Gembloux
Agro-Bio Tech

Assessing Above Ground Biomass C-storage in Bamboo (Belgium)

Guillaume BERNARD

THESIS PRESENTED FOR THE OBTAINING OF A DEGREE IN
BIOENGINEERING IN ENVIRONMENTAL SCIENCES AND TECHNOLOGIES

ACADEMIC YEAR 2022 - 2023

CO-PROMOTERS: Pr. Jeroen MEERSMANS, Pr. Tom DE MIL

Host institutions

This thesis was carried out at the Gembloux Agro-Bio Tech Faculty of the University of Liège, in the Water-Soil-Plants Exchange Department. The external host organisation for the field measurements was the botanical garden "De Kleine Boerderij".

Acknowledgememt

First, i would like to thank my two promotors Jeroen Meersmans and Tom De Mil for giving me to opportunity to work on this interesting subject. You showed me great guidance and i feel privileged to have had the opportunity to work with such esteemed professionals who genuinely care about their students' success.

Thanks to Mr.Oprins for his availability and responsiveness. It is an honor and a chance that you gave me the opportunity to study the bamboos from "De Kleine Boerderij".

Thanks to my field trip collegua's, Claire, Hélène, Nahama and Pierre. You have been a great help and you made my long days on the field such great memories. And thanks to all the people who have helped me one way or another during this long processus.

Thanks to Nicolas Kovacs for his kind attitude and his precious help during the entirety of this work.

Thanks to all my close friends for the great memories we made during those beautiful but long years at Gembloux Agro-bio Tech.

Thanks to my dear family for sticking up with me in these particularly hard times. Especially my sister Camille and my aunt Chantal.

Finally, thanks to my lovely girlfriend Hélène for her unconditional support. I couldn't have come this far without her.

Abstract

Bamboo, is a rapidly growing and versatile plant. Over the last years, it has gained significant attention as a potential resource for carbon sequestration and climate change mitigation strategies. Despite its global presence, bamboo's role in carbon stock assessment remains underexplored, particularly within the context of European climates. This study aims to address this research gap by conducting a comprehensive assessment of bamboo's carbon stocks in 3 *Phyllostachys* species in Merksplas (Belgium). The study was initiated by surveying the bamboo stands to analyze the distribution of Diameter at Breast Height (DBH) and design a representative sampling plan. Once the needed data was collected, various regression methods were tested using a combination of different input variables (DBH,H, and basic density). Based on model performance metrics (R^2, R^2_{adj}, AIC, RMSE, MAPE)The best regression equations were then rigorously cross-validated with Monte-Carlo Cross-Validation to ensure their accuracy across a larger panel. Using the validated equations, Above-Ground Biomass (AGB) and Above-Ground Carbon (AGC) were estimated. They returned values ranging from 9.48 ± 1.19 to 52.36 ± 4.26 $tonAGB{\cdot}ha^{-1}$ and 4.45 ± 0.56 to 24.61± 2.00 $tonC{\cdot}ha^{-1}$. Additionally, the growth of new bamboo shoots was measured to gauge the annual carbon sink. This returned estimations from 0.51 ± 0.12 and 2.96 ± 0.21 $tonC{\cdot}ha^{-1}$. Overall, the approach provides a comprehensive assessment of bamboo's role as a carbon sink and stock in Belgium's climate. By integrating field data collection, regression analysis, cross-validation, and shoot growth measurements, it enhance the understanding of bamboo's contribution to mitigating climate change in European climatic contexts. In addition, allometric equations were developed and with caution, they could be utilized by other researchers. These equations offer a potential tool for estimating carbon stocks in similar contexts.

Keywords : Climate change mitigation - Belgium - Bamboo - Carbon stock - Allometric equations - Above-Ground Biomass (AGB) - *Phyllostachys*

Résumé

Le bambou est une plante versatile à croissance rapide. Au cours des dernières années, il a suscité un intérêt considérable en tant que ressource potentielle pour la séquestration du carbone et les stratégies d'atténuation du changement climatique. Malgré sa présence globale, le rôle du bambou dans l'évaluation des stocks de carbone reste peu exploré, en particulier dans le contexte des climats européens. Cette étude vise à combler cette lacune en réalisant une évaluation complète des stocks de carbone du bambou dans trois espèces de *Phyllostachys* à Merksplas (Belgique). L'étude a démarré en enquêtant sur les peuplements de bambous pour analyser la distribution du diamètre à hauteur de poitrine et concevoir un plan d'échantillonnage représentatif. Une fois les données nécessaires collectées, différentes méthodes de régression ont été testées en utilisant une combinaison de différentes variables d'entrée (DBH, H et densité de base). Sur la base des mesures de performance du modèle (R^2, R^2_{adj}, AIC, RMSE, MAPE), les meilleures équations de régression ont ensuite été rigoureusement validées avec une validation croisée de Monte-Carlo pour garantir leur précision sur un large échantillon. À l'aide des équations validées, la biomasse aérienne et le carbone aérien ont été estimés. Ils ont renvoyé des valeurs allant de 9,48 ± 1,19 à 52,36 ± 4,26 $tonneAGB{\cdot}ha^{-1}$ et de 4,45 ± 0,56 à 24,61 ± 2,00 $tonneC{\cdot}ha^{-1}$. De plus, la croissance des nouvelles pousses de bambou a été mesurée pour évaluer le puits de carbone annuel. Cela a donné des estimations allant de 0,51 ± 0,12 à 2,96 ± 0,21 $tonneC{\cdot}ha^{-1}$. Dans l'ensemble, cette approche offre une évaluation complète du rôle du bambou en tant que puits et stock de carbone dans le climat belge. En intégrant la collecte de données sur le terrain, l'analyse de régression, la validation croisée et les mesures de la croissance des pousses, elle améliore la compréhension de la contribution du bambou à l'atténuation du changement climatique dans les contextes climatiques européens. De plus, des équations allométriques ont été développées et pourraient être utilisées avec prudence par d'autres chercheurs. Ces équations offrent un outil potentiel pour estimer les stocks de carbone dans des contextes similaires.

Mots-clés : Atténuation du changement climatique - Belgique - Bambou - Stocks de carbone - Équations allométriques - Biomasse aérienne - *Phyllostachys*

Table of contents

List of Figures

List of Tables

Acronyms

R^2 Coefficient of Determination.
ρ Basic Density.
$\boldsymbol{CH}_4$ Methane.
$\boldsymbol{CO}_2$ Carbon Dioxide.
$R^2_{\mathbf{adj}}$ Adjusted Coefficient of Determination.
$\boldsymbol{ppm}$ Parts per million.
AGB Aboveground Biomass.
AGB Aboveground Biomass.
DBH Diameter at Breast Height.
GHG Greenhouse Gas.
GWP Global Warming Potential.
INBAR International Bamboo and Rattan Organization.
MAPE Mean Absolute Percentage Error.
MCCV Monte-Carlo Cross-Validation.
RMSE Root Mean Squared Error.

I Introduction

1 Context

Climate change is an urgent matter to tackle. It is now well known that Greenhouse Gas (GHG) emissions, produced by human activities, cause global warming (IPCC, 2023). Carbon dioxide (CO_2)and methane (CH_4) are the two main anthropogenic GHGs emitted into the atmosphere. They are followed by Nitrous Oxide, Sulfur Dioxide and fluorinated gasses. In 2019, CO_2 emissions represented 76 % of the GHG emissions while Methane emissions were 13 %. Atmospheric CO_2 concentration has continuously risen. It was approximately 278 parts per million (ppm) in 1750, 300 ppm in the 1910s, 350 ppm in the late 1980s, and almost 420 in 2023 (Dlugokencky & Tans, 2023; Friedlingstein et al., 2022). The primary sources of CO_2 are fossil fuel combustion and deforestation. Methane is produced mainly by biomass combustion and agricultural wastes (Yoro & Daramola, 2020). Although CH_4 represents less emissions than CO_2, it is estimated to have a global warming potential (GWP) more than 20 times superior to CO_2 (UNFCCC, n.d.). GWP is a metric that helps to facilitate comparison by normalizing GHG fluxes as CO_2 equivalent. This metric has been used globally since the Kyoto Protocol.

The Kyoto Protocol was signed in 1997 and went into operation in 2005. It represents the first global and legal practical implementation aiming to reduce GHG emissions. After the Kyoto Protocol came the Paris Agreement. It was adopted in 2015 and is a legally binding international treaty. It aims to hold the global temperature increase below 2°C from preindustrial levels and to ideally limit the temperature increase to 1.5°C above preindustrial levels. Those two events have led to the creation of new markets and opportunities. Furthermore, since the adoption of the Paris Agreement in 2015, a diminution of CO_2 emissions of 0.8 % has been observed in developed countries (on average between 2016-2019 compared to 2011-2015) (Le Quéré et al., 2021). In the continuity of the Paris Agreement, the latest Conference of the Parties(COP27), held at Sharm el-Cheikh, *"Recognizes that limiting global warming to 1.5 °C requires rapid, deep and sustained reductions in global greenhouse gas emissions of 43 per cent by 2030 relative to the 2019 level"* (UNFCCC, 2023).

Multiple solutions exist to mitigate climate change. The literature describes three main types of climate mitigation approaches (Fawzy et al., 2020). Firstly, conventional methods are those that use decarbonization techniques and the ones that reduce CO_2 emissions. Examples are nuclear energy, renewable energies, efficiency gains, etc. Those are technologies and methods that are well established and are being improved. Secondly, there are new sets of technologies and methods that aim to sequester carbon that is already in the atmosphere. A few examples discussed in the literature are biochar, soil carbon sequestration, afforestation and reforestation, wetland construction and restoration. These are nature-based solutions. On the other hand, industrial solutions mainly consist of absorption, adsorption, chemical looping and membrane-use techniques (Al-Mamoori et al., 2017). These technologies can be called negative emissions technologies (Ricke et al., 2017). Thirdly, new technologies have been developed with the objective to influence the solar and terrestrial radiations. These techniques are called radiative forcing engineering and their aim is to manipulate the temperature without a modification in GHG in the atmosphere. These techniques are still in their early days and a lot of uncertainties remain, especially on large scales. They also raise questions over ethics and governance dilemmas (Lawrence et al., 2018).

Due to their long-term horizon, forestry investments have long been seen as risky. However, during the years, knowledge has been acquired on forestry projects related to carbon fixing in the long term (Van Der Gaast et al., 2018). According to the last IPCC Report (IPCC, 2021), ecosystem restoration, afforestation and reforestation can reach a potential contribution to net emissions reduction of up to almost 3 $GtCO_2\text{-}eq/yr$ (Gigatone of CO_2 equivalent per year) by 2030. But the report also states that the implementation of these mitigation techniques at this level could cost up to 100–200 USD (US Dollar) per $tCO_2\text{-}eq$ (Ton of CO_2 equivalent per year). The potential revenue available through the sale of carbon credits could help to reduce the costs (Hou et al., 2019).

Because of their biological characteristics and growth, bamboos have interesting properties regarding soil erosion control, water conservation, land rehabilitation, and carbon sequestration (Ben-zhi et al., 2005). A review of the literature on carbon fixation in bamboo forests in China led to the conclusion that this type of forest may be one of the most interesting regarding carbon sequestration (Zhou et al., 2011). Given the afore-described context, bamboo could thus be a potential response to climate change mitigation.

2 Carbon Dynamics

When it comes to the global carbon budget, there are four major carbon reservoirs: the atmosphere, the oceans, the terrestrial ecosystems (vegetation and soils) and the fossil fuels (Houghton, 2007). Terrestrial ecosystems play a crucial role in the global carbon cycle by absorbing and storing carbon dioxide from the atmosphere through photosynthesis. The carbon dynamics of terrestrial ecosystems involve the movement and storage of carbon within different pools, such as vegetation, soil, and the atmosphere. In terrestrial ecosystems, the amount of carbon stored in soil is estimated to be greater than the amount stored in vegetation and atmosphere (Scharlemann et al., 2014). But terrestrial vegetation is a central component of the global carbon cycle. In the latest global carbon budget (Friedlingstein et al., 2022), it is estimated to stock 450 GtC (Figure 1).

The definition of the carbon balance of an ecosystem at any point in time is the difference between carbon gains and carbon losses. In short, terrestrial ecosystems gain carbon thanks to photosynthesis and lose it in the forms of CO_2 during the respiration of autotrophs and heterotrophs organisms. If photosynthesis is greater than respiration,

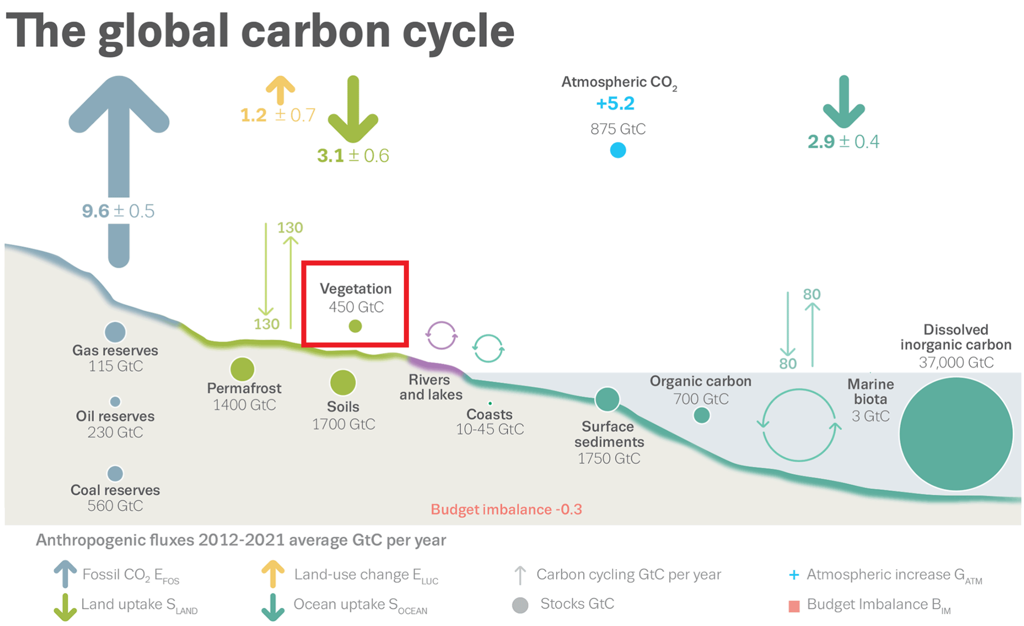

Figure 1: The global carbon cycle (Friedlingstein et al., 2022), and the role of vegetation uptake therein

the ecosystem is a net carbon sink, meaning that it is storing carbon. If respiration is greater than photosynthesis, the ecosystem is a net carbon source, meaning that it is releasing carbon. Those two actions lead to a modification in carbon stocks. Ultimately, the long-term capture and storage of carbon from the atmosphere is called carbon sequestration (Keenan & Williams, 2018). From one year to another, ecosystems can turn from sink to source and vice-versa, so an ecosystem needs to be a sink on longer timelines for it to sequester carbon.

Ecosystems are dependent on local climatic conditions, suggesting various climate ecosystem feedbacks (Heimann & Reichstein, 2008). Keenan and Williams (2018), classify the main drivers of terrestrial carbon sink in four different categories. Firstly, there are the direct climate effects i.e. the changes in precipitation, temperature (Yuan et al., 2011) and radiation regime (Pan et al., 2011). Secondly, there is the atmospheric composition and its effects, such as CO_2 fertilization (Norby et al., 2005), nutrient deposition and pollution damage. Thirdly, there are the effects induced by land-use changes, for example, deforestation, afforestation and agricultural practices. And lastly, natural disturbance effects also need to be accounted for: hurricanes, high winds, wildfire, pests and pathogens.

3 Bamboo as an Effective Carbon Sequestration Solution

Bamboo, with its ability to grow rapidly and persist for long periods without causing a substantial reduction in culm stock after harvesting, has emerged as one of the most promising species for carbon storage and sequestration. Due to a rising interest in this solution, multiple studies have reported on the rate of above ground biomass and Carbon stock potential in bamboo (Li et al., 2015; Nath et al., 2015; Song et al., 2011; Yuen et al., 2017; Zhou et al., 2011).

The carbon sequestration potential of bamboo is due to several factors. First, bamboo is considered to be one of the fastest growing plants in the world. Depending on species, it can grow between 3 and 30 m in the span of 3-4 months (Kleinhenz & Midmore, 2001). Depending on management practices and bamboo species, it is said that bamboo can be harvested every 3-5 years. This gives bamboo the potential to store carbon on a short period of time. Secondly, bamboo can grow in a large variety of soil and in various climatic conditions. This versatility provides bamboo with the ability to grow in many different parts of the world. Thirdly, with efficient management, bamboo can be harvested regularly without clearing the land (Kuehl et al., 2013). Finally, bamboo as a long lifespan. This mean that with efficient management, it can store carbon in the long term. Furthermore, the bamboo industry is continuously developing, making bamboo products a great option for carbon sequestration in the near future(Gielis, 2023; Xu et al., 2022).

Trough the use of allometric equations, AGB and C stocks in bamboo can be estimated precisely, everywhere, and in any condition. Many recent studies have developed different allometric equations for bamboo species (see in appendix, Figure26). These studies were mainly conducted in Asia and South America but they have not yet been carried out in Europe.

4 Bamboo: A Botanical Overview

Bamboo is a widely spread species. It is classified among the subfamily *Bambusoideae* from the grass family *Poaceae*. The last updated classification indicates that there are 1698 different species divided in 136 genera (Soreng et al., 2022). It is also separated into three different tribes: *Arundinarieae* (temperate woody bamboos), *Bambuseas*(tropical woody bamboos), and *Olyreae*(herbaceous bamboos). In 2020, it was estimated that bamboo covered about 35 million hectares on earth (FAO, 2020a). This signifies that bamboo covers about 3.2 % of the total world forest area (Troya Mera & Xu, 2014). Native species can be found principally in Asia, America and Africa (Ahmad et al., 2021). No species are endemic from Europe (or Antarctica) but, a lot of them were successfully introduced and cultivated in Europe. The distribution of bamboo plants is based on a particular set of conditions like rainfall, soil type, temperature and altitude. Bamboos prefer zones where the annual rainfall ranges from 1200 to 4000 mm and the annual average temperature oscillates between 8 to 36 °C. They easily grow in soil types like sandy soils, loamy soils, hard lateritic soils and rich alluvium soils. Bamboos are usually located between 47° S to 50° 30 N in latitude and from sea level to 4300 m above (Judziewicz et al., 1999, Ohrnberger 1999, Soderstrom and Calderon 1979, all cited by Liese and Köhl, 2015).

Bamboo's anatomical structure defines its properties. Bamboo is botanically a grass, which unlike trees, only produces a primary shoot and does not go through secondary growth.

However, the FAO defines a tree as *"a woody perennial with a single main stem, or in the case of coppice with several stems, having a more or less definite crown. It includes bamboos, palms, and other woody plants meeting the above criteria."* (FAO, 2020b). Bamboo has two major parts, the culm (stem) and the rhizomes. The culm of the bamboo consists of nodes and internodes (Figure 2). In the majority of species, the internodes are surrounded by a culm wall of variable length. The gap in that internode is called the lacuna. Rhizomes store the nutrients needed for growth and secure the bamboo into the ground (Akinlabi et al., 2017). The development of new culms occurs in parts : the shoots first emerge to their full length bearing culm leaves; then, there is the culm lignification with branch development on the internodes and production of foliage leaves(Liese & Köhl, 2015).

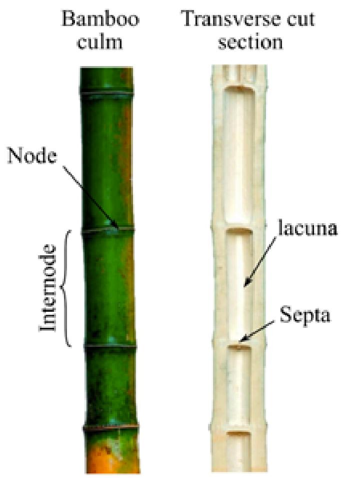

Figure 2: Bamboo culm and transverse section morphology (Gangwar & Schillinger, 2019)

There are two main types of bamboos: clumping, also known as sympodial or pachymorph, and running, also known as monopodial or leptomorph (Figure 3). The clumping type is generally of tropical or subtropical provenance and cannot support freezing temperature. The running type can support occasionally low temperatures (Mera & Xu, 2014). The most important genus of temperate climate species, *Phyllostachys*, belongs to that second category.

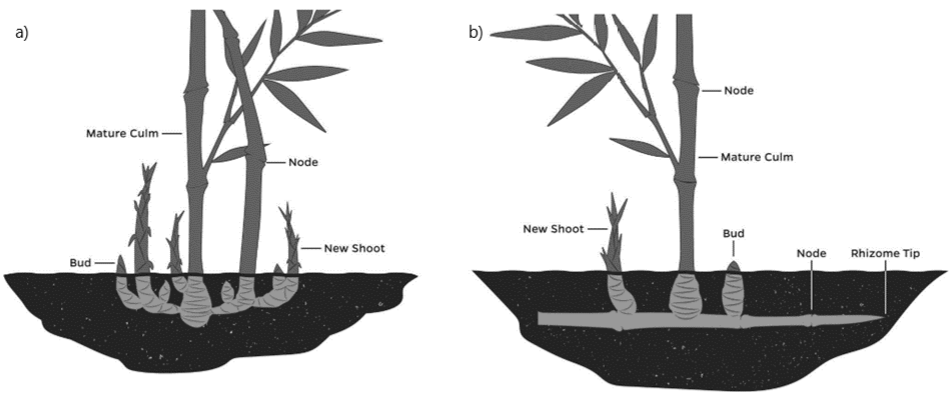

Figure 3: Rhizome structure of clumping (a) and running (b) bamboo (Lieurance et al., 2018).

The *Phyllostachys* genus is from the Tribe *Arundinarieae*. A few characteristics from the tribe is that the rhizomes are well developed with some taxa with only pachymorph ones, the culms are woody and usually hollow and the branch development starts from the apex to the base. They are mainly distributed in forests of the northern temperate zone, sometimes also in high elevation tropical regions of both hemispheres (Liese & Köhl, 2015). Due to the fact that it is usually grown in plantations for commercial uses, *Phyllostachys Pubescens*, or *Moso Bamboo*, is the most studied bamboo species with more than 40 % of the reported values (Yuen et al., 2017). In this paper, 3 other *Phyllostachys* bamboos are studied : *Phyllostachys Aurea* (*P.Aurea*), *Phyllostachys Aureosulcata* (*P.Aureosulcata*) and *Phyllostcahys Nigra* (*P.Nigra*). All three species are running type and are not native to Belgium and Europe. Their complete taxonomy (Vorontsova et al., 2016b) and known distribution (Vorontsova et al., 2016a) can be found in Appendix B.

Phyllostachys Aurea is also called green bamboo or gold bamboo. It is primarily cultivated for its ornamental use. It has a green culm that can turn golden depending on age and sun exposure (Figure 4a). It has an evergreen green foliage. It also shows the particularity of compressed internodes at the basis of the culm (Figure 4b). Its diameter measures around 5 *cm* and its height varies between 7 and 9 *m* (Liese, 1985 cited by Liese and Köhl, 2015).

(a) (b)

Figure 4: Picture of *Phyllostachys Aurea* plantation in Merksplas (a), and picture of compressed internodes (b).

Phyllostachys Aureosulcata is also called Yellow bamboo (Figure 5). It is cultivated mainly for ornamental use but his shoots are also edible. It possesses a striped yellow and green culm. Its diameter measures around 4 *cm* and its height can grow to 9 *m* (*Phyllostachys aureosulcata* McClure, J. Wash. Acad. Sci. 35: 282. 1945, cited by "Flora of China: Bambusoideae", n.d.).

Figure 5: Picture of *Phyllostachys Aureosulcata* plantation in Merksplas.

Phyllostachys Nigra is also called Black bamboo. It is cultivated for ornamental use. Young culms are greenand then they turn into a unique black color (Figure 6). This special feature makes it one of the most popular garden bamboo (Liese & Köhl, 2015). Its diameter measures around 2-3 cm and Its height varies between 5 and 7 m (Liese, 1985 cited by Liese and Köhl, 2015).

Figure 6: Picture of *Phyllostachys Nigra* plantation in Merksplas.

5 Objectives of Study

It is clear that climate change mitigation techniques have gained attention over the last few years. Studies on the subject are numerous and indicate that bamboo could represent a great opportunity for carbon sequestration. However, the majority of scientific research in this field has been done mostly in Asia, and on a small set of bamboo species. For this reason, there is lack of knowledge regarding temperate species carbon sequestration potential in Europe.

The present work, therefore, aims to:

(i) Create and evaluate AGB estimation models of 3 *Phyllostachys* species (*Phyllostachys Aurea, Phyllostachys Aureosulcata, Phyllostchys Nigra*) in the climatic context of Northern Belgium.

(ii) Characterize and compare the potential regarding carbon stocks and sequestration of the said bamboo species.

(iii) Explore the yearly Carbon sink potential of the three species.

II Materials and methods

1 Study Site

The experiment took place in the botanical garden De Kleine Boerderij. It is located in Merksplas, a small municipality in northern Belgium (51°20'53"N, 4°49'38"E). The plantation there has no commercial or production purpose, but the bamboos are periodically managed (selective cutting, pruning, cutting of other species,...). On site, three different plots were selected, each one of them being covered by one species (Figure 7). These plots were chosen based on accessibility and because of the clear identification of the species.

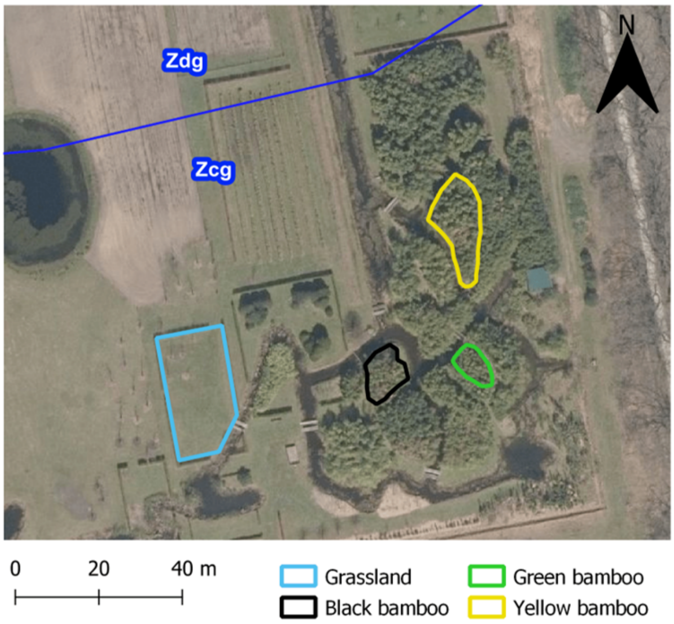

Figure 7: Bamboo plots in Merksplas (Kovacs, 2022)

2 Climate

The climate there is temperate. From data collected by the Royal Meteorological Institute of Belgium (RMI, Royal Meteorological Institute of Belgium, n.d.) between 1991 and 2020, the average temperature over the year in Merksplas is 10.8°C, and the average annual precipitation is 893.5 *mm*. The average maximum temperature (23.6°C) occurs during the summer, which runs from June to September, while the average minimum temperature (0.8°C) occurs during the winter, which runs from December to March.

3 Equipment

i Field measurement and manipulations

For the three sites, culms were marked, counted and Diameter at Breast Height (DBH) i.e. 1.3 *m* where measured. Additionally, leaf nets were installed in an attempt to measure leaf fluxes (Devi & Singh, 2021). In order to facilitate comparison, the pH of the plots was estimated (Huy & Long, 2019). Then, in order to have an estimate of the yearly sink, new shoots were counted and measured (DBH and height).

Culms counting and marking, DBH and Height measurements. Every culm of each plot was marked and numbered with a permanent marker. The culms located near the border of each plot (at 1 *m*) were also attributed the letter B. Every culm DBH was measured and a smaller proportion (+-10%) of culm heights was measured. The DBH measurements were made with two different calipers. The first one was a mechanical caliper with a precision of 1 *mm*. The second one was a digital caliper with a precision of 0.01 *mm*. Values measured with the electronic caliper were rounded to the *mm*. The heights (H) were estimated with the help of a logger's tape and a stick.

Soil pH. A pH kit (Pehameter Modell HELLIGE from AVM) was used to characterize soil pH on site. Soil litter was taken out and an auger was used to remove the 10 first *cm* of the soil for the test to be made on soil sampled at a depth of 10 *cm*.

Leaf nets. Leaf nets of 50 by 50 *cm* were built and placed on site at 50 *cm* above ground (Figure 8). One leaf net was placed on the Black Bamboo plot, one on the Green Bamboo plot and 3 on the Yellow Bamboo plot.

Figure 8: Leaf net number 2 on *P.Aureosulcata* plot.

New shoots counting and measurements. At the beginning of July 2023, new shoots were counted and measured. DBH was measured with the electronic caliper (measured precision was 0.01 *mm*) and heights were estimated with the help of a logger's tape and a stick.

Sampling and samples treatment. Selected culms were harvested with a pruning saw and height was measured with a precision of 0.1 *m*. They were then transported back to the laboratory where they were roughky cut and put in labelled lock bags. The culms, branches, and leaves were then separated and put back in lock bags. Culms were cut in final smaller parts with a bandsaw to split the lower, middle and higher parts and to separate nodes and internodes. Once cut, inner and outer diameter of 3 culms parts (basal, DBH and 1 *m* higher).

ii Laboratory measurements and manipulations.

Dry biomass measurements. According to International Bamboo and Rattan Organization (INBAR) methodology (Huy & Long, 2019), culms, branches and leaves should each be separated into subsamples of +- 100-300 *gr* each (3 subsamples for the culm: base, middle and top). However, the bamboos analyzed in this study are small. Therefore most of the sampled bamboos have been analyzed in totality, with the exception of a few larger specimens.

Once all the parts were separated they were weighted to obtain fresh mass. To obtain dry mass, the samples went into the oven at 105C° for 48H. It was then possible to obtain the fresh-to-dry ratio and calculate the total dry weight (1).

$$\mathrm{TDW} = \mathrm{TFW} \times \frac{\mathrm{SDW}}{\mathrm{SFW}} \tag{1}$$

where:

$$\begin{aligned}
TDW &: \text{Total Dry Weight} \\
TFW &: \text{Total Fresh Weight} \\
SDW &: \text{Sample Dry Weight} \\
SFW &: \text{Sample Fresh Weight}
\end{aligned}$$

Basic Density. When cut and while fresh, culm sample volumes were measured by submersion. This manipulation is based on Archimedes principle (Figure 9). A recipient filled with distilled water is placed on an electronic scale. Inside the recipient is also placed a physical support sustained thanks to a laboratory stand that is next to the scale. The object whose volume we want to measure is dipped in the water (laid on the support or blocked below the support depending on density). The difference in mass induced on the electronic scale translates the displaced volume. Due to the hollow form of bamboo nodes and internodes, great care must be taken to expel air bubbles.

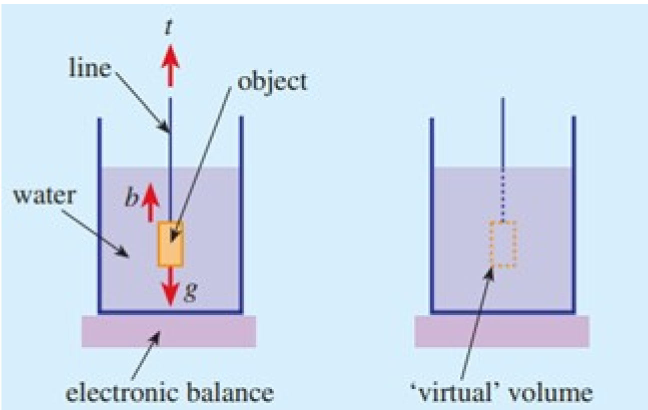

Figure 9: Schema of volume measurement based on Archimedes Principle (Hughes, 2005).

With the fresh volumes and the dry masses, basic density (ρ) can be calculated (2) :

$$\text{Basic Density} = \frac{\text{Oven-Dry Mass (g)}}{\text{Green Volume (cm}^3\text{)}} \tag{2}$$

4 Sampling Plan

In an attempt to limit the number of sampled culms, it was decided to sample 10 culm of each species. For each species, the distribution was studied. Based on those distributions, one culm was sampled in each decile (Table 1). This method aims to represent all the distributions with a limited sample number. It is also similar to the UNFCCC guidelines when a small number of samples are used for the modelisation of allometric equation (UNFCCC, 2011).

Table 1: Deciles separation of the DBH distribution in *mm* for the 3 *Phyllostachys* species.

	10%	**20%**	**30%**	**40%**	**50%**	**60%**	**70%**	**80%**	**90%**
P.Aurea	8.00	11.00	13.00	14.00	16.00	17.00	19.00	21.00	25.00
P.Aureasulcata	15.00	18.00	20.00	22.00	25.00	26.00	28.00	32.00	38.40
P.Nigra	8.00	11.00	13.00	15.00	17.00	19.00	21.00	24.00	26.00

5 Modelling

A multitude of allometric models to predict Aboveground Biomass (AGB) were tested using different input variables, formulas and regression methods. Those models were then compared to each other with the help of various model performance metrics. Ultimately, the models with the best fit were tested using cross validation.

i Data

Due to the small dataset (30 samples, 10 of each species) the modelling was first done with a multispecies model (i.e. lumping all species together). Then each species was modeled individually.

ii Input Variables

In the literature, the parameters that were most often used to predict bamboo AGB were DBH and height (Huy et al., 2019; Li et al., 2016; Yen et al., 2010; Yuen et al., 2017). Other studies (Chave et al., 2005; Picard et al., 2015) also pointed out the importance of adding basic density (ρ) into regression models for trees in the tropics area to obtain a more accurate estimation. This input will also be tested in this study. Globally, the relations tested are of the form:

$$AGB = f(D, H, \rho) \tag{3}$$

Where:

$$\begin{aligned} AGB &: \text{Above Ground Biomass (in } kg\text{)} \\ D &: \text{Diameter at Breast Height (in } cm\text{)} \\ H &: \text{Height (in } m\text{)} \\ \rho &: \text{Basic Density (in } g/cm^3\text{)} \end{aligned}$$

iii Linear and Nonlinear Regression Modelling

Due to relations between predictor and the response of biomass often being non-linear and heteroscedastic, the use of weighted variables is of primordial importance (Huy & Long, 2019). Depending on the model and the data, multiple weighing methods have been tested. Two types of regression will be tested: linear and non-linear.

Based on experimentation, it is known that the power model can be fit by using log-transformed data linear regression (Basuki et al., 2009; Chave et al., 2014). It then takes this form:

$$\log(AGB) = a + b \times \log(D) + c \times \log(H) + d \times \log(\rho) \tag{4}$$

It can also be fit as a non-linear mode (Huy et al., 2016b; Poudel & Temesgen, 2016) (5):

$$AGB = a \times D^b \times H^c \times \rho^d \tag{5}$$

Linear Regression. Linear regression is a fundamental statistical method used to model the relationship between a dependent variable and one or more independent variables. The goal of linear regression is to fit a straight line (in the case of one independent variable) or a hyperplane (in the case of multiple independent variables) that best represents the relationship between the variables. This line or hyperplane is used to make predictions about the dependent variable based on the values of the independent variable(s).

The goal of linear regression is to estimate the coefficients a,b,c,d (in equation 4) that best fit the data. The most common approach used to estimate these coefficients is the method of least squares. This method aims to find the best-fitting line or hyperplane through the data by minimizing the sum of the squared differences between the observed and predicted values of the dependent variable. These squared differences are often referred to as "residuals".

Nonlinear Regression. In contrast to linear regression, which assumes a linear relationship between the variables, nonlinear regression allows for more flexible and complex relationships by using nonlinear equations to fit the data. In nonlinear regression, the objective is to estimate the values of the parameters a,b,c,d (in equation 5) that best fit the data. This process involves finding the set of parameters that minimizes the sum of squared residuals, similar to the method of least squares used in linear regression. However, due to the nonlinearity of the function, the optimization of the objective function becomes more complex and often requires iterative numerical methods.

iv Model Quality

Assessing the quality of the models is primordial (Chave et al., 2005; Huy et al., 2016a; Mayer & Butler, 1993; Poudel & Temesgen, 2016). A lot of different models have been tested and the following model performance metrics have been chosen to estimate their quality and select the best of them.

Coefficient of determination - R^2. The coefficient of determination, or R-squared (R^2) parameter, is a statistical measure that quantifies the proportion of the variance in the dependent variable that is predictable from the independent variables in a regression model. It is used to evaluate the goodness-of-fit of the regression model to the data:

$$R^2 = 1 - \frac{\sum_{i=1}^{n}(AGB_i - A\hat{G}B_i)^2}{\sum_{i=1}^{n}(AGB_i - A\bar{G}B)^2} \tag{6}$$

Where:

R^2 : Coefficient of determination
n : Number of data points
AGB_i : Observed aboveground biomass for the ith data point
$A\hat{G}B_i$: Predicted aboveground biomass for the ith data point based on the model
$A\bar{G}B$: Mean of the observed aboveground biomass values

R^2 ranges from 0 to 1, where 0 indicates that the model explains none of the variability, and 1 indicates that the model explains all of the variability. A higher R-squared value suggests a better fit of the model to the data, as it indicates that a larger proportion of the variance in the dependent variable is explained by the regression model.

Adjusted coefficient of determination - R^2_{adj}. Adjusted coefficient of determination or R-squared adjusted (R^2_{adj}) is a modification of the regular R^2 value used in multiple linear regression. While R-squared represents the proportion of the variance in the dependent variable that is explained by the independent variables in the model, R-squared adjusted takes into account the number of independent variables in the model to provide a more balanced evaluation of the model's goodness-of-fit:

$$R^2_{\text{adj}} = 1 - \frac{(1 - R^2) \cdot (n - 1)}{n - k} \tag{7}$$

Where:

$$
\begin{aligned}
R^2_{\text{adj}} &: \text{Adjusted coefficient of determination} \\
R^2 &: \text{Coefficient of determination} \\
n &: \text{Number of data points} \\
k &: \text{Number of independent variables (predictors) in the model}
\end{aligned}
$$

The key difference between R^2_{adj} and R^2 adjusted is the penalty term. This penalty term adjusts the R-squared value based on the number of independent variables used in the model. If the number of independent variables increases, the penalty becomes more significant. This would lead to a reduction in the R-squared adjusted value compared to the regular R-squared value.

R^2_{adj} is useful when comparing models with different numbers of independent variables. It provides a more conservative evaluation of model fit by taking into account the potential overfitting that can occur when adding more predictors. Generally, a higher R-squared adjusted value indicates a better balance between the model's complexity and its fit to the data.

Akaike Information Criterion - AIC .
AIC stands for Akaike Information Criterion. It is a statistical measure used for model selection in the context of regression analysis and other statistical modeling techniques. The AIC provides a way to compare different models and select the one that best balances goodness of fit and model complexity (Akaike, n.d.; Cavanaugh & Neath, 2019). In general, the AIC estimates the relative quality of a model based on how well it fits the data and the number of parameters used in the model. It is calculated using the following formula :

$$\text{AIC} = 2k - 2\ln(L) \tag{8}$$

Where:

$$
\begin{aligned}
\text{AIC} &: \text{Akaike Information Criterion} \\
k &: \text{Number of estimated parameters in the model} \\
L &: \text{Maximum likelihood value of the model}
\end{aligned}
$$

The AIC penalizes models with more parameters, and favors those that fit the data well but use fewer parameters. This penalty discourages overfitting, as adding unnecessary parameters to the model may improve the fit to the training data but may not generalize well to new data. When comparing different models, a lower AIC value indicates a better balance between goodness of fit and model complexity, and the model with the lowest AIC is considered the best model among the candidate models. It is important to note that AIC is a relative measure, meaning that the absolute value of AIC does not carry any meaning by itself. Only the comparison of AIC values between different models is meaningful for model selection.

Bias. Bias refers to the difference between the average prediction of a model and the true value it is trying to predict. More specifically, it is the systematic error introduced by the model due to its inability to capture the true underlying relationship between the input variables and the output variable. The formula is the following :

$$\text{Bias }\% = \frac{100}{n}\sum_{i=1}^{n}\frac{AGB_{\text{predicted},i} - AGB_{\text{observed},i}}{AGB_{\text{observed},i}} \tag{9}$$

Where:

$$\begin{aligned}
\text{Bias }\% &: \text{Bias percentage} \\
n &: \text{Number of data points} \\
AGB_{\text{observed},i} &: \text{Observed aboveground biomass for the } i\text{th data point} \\
AGB_{\text{predicted},i} &: \text{Predicted aboveground biomass for the } i\text{th data point}
\end{aligned}$$

If the bias is close to zero, it indicates that, on average, the model predictions are unbiased. A positive bias suggests that, on average, the model tends to underpredict the true values, while a negative bias indicates that it tends to overpredict the true values.

Root Mean Squared Error - RMSE. Root Mean Squared Error (RMSE) is a commonly used metric to evaluate the performance of a predictive model, particularly in the context of regression analysis. RMSE measures the average prediction error of the model by calculating the square root of the mean of the squared differences between the model's predicted values and the actual observed values. The formula to calculate RMSE is as follows:

$$\text{RMSE} = \sqrt{\frac{1}{n}\sum_{i=1}^{n}(AGB_{\text{predicted},i} - AGB_{\text{observed},i})^2} \tag{10}$$

Where:

$$\begin{aligned}
\text{RMSE} &: \text{Root Mean Square Error} \\
n &: \text{Number of data points} \\
AGB_{\text{observed},i} &: \text{Observed aboveground biomass for the } i\text{th data point} \\
AGB_{\text{predicted},i} &: \text{Predicted aboveground biomass for the } i\text{th data point}
\end{aligned}$$

RMSE measures the differences between the predicted values and the actual values in the same units as the dependent variable. It penalizes large errors more heavily, as errors are squared before taking the mean and then the square root. A lower RMSE value indicates that the model's predictions are closer to the actual values, suggesting better predictive performance.

Mean Absolute Percentage Error - MAPE. Mean Absolute Percentage Error (MAPE) is a metric used to evaluate the accuracy of a model's predictions in percentage terms. It measures the average percentage difference between the model's predicted values and the actual observed values. The formula to calculate MAPE is as follows:

$$\text{MAPE} = \frac{1}{n} \sum_{i=1}^{n} \left| \frac{AGB_{\text{predicted},i} - AGB_{\text{observed},i}}{AGB_{\text{observed},i}} \right| \times 100\% \tag{11}$$

Where:

$$\begin{aligned} \text{MAPE} &: \text{Mean Absolute Percentage Error} \\ n &: \text{Number of data points} \\ AGB_{\text{observed},i} &: \text{Observed aboveground biomass for the } i\text{th data point} \\ AGB_{\text{predicted},i} &: \text{Predicted aboveground biomass for the } i\text{th data point} \end{aligned}$$

MAPE calculates the absolute percentage error for each data point, and then takes the average of these absolute percentage errors to provide an overall measure of the model's prediction accuracy in percentage. MAPE is used to compare the performance of different models, especially when the magnitude of the dependent variable is high. It gives a percentage representation of the average prediction error, which is sometimes more interpretable and easier to communicate than other model metrics.

v Cross-validation

The cross-validation step is needed to ensure that the model works in a more general way and that it is not overfitted to the training data. Here, the cross validation technique used is the Monte-Carlo Cross-Validation (MCCV). This choice was made because it is a recommended technique if there is a small number of samples in the dataset. In addition, MCCV is also frequently used in Bamboo AGB modelling (Huy et al., 2019).

With MCCV the data is randomly partitioned into training and validation sets for each iteration. Here, we used an 80/20 or 70/30 % division. The process is repeated multiple times, here 200 times for the larger set and 50 times for the smaller sets, with different random partitions in each iteration. After each iteration, the performance metric is recorded, and the final performance estimate is calculated as the average of the performance metrics over all iterations.

6 Aboveground Biomass and Carbon Stocks estimation

Once validated models are obtained. They are used to estimate Aboveground Biomass and C stock for each species and for the 3 combined. This is done for the adult culms but also for the young shoots measured in July. To obtain those results, bamboo data (D and H) are put into a Monte-Carlo Simulation with a high numbers of iterations (1000). This return the mean AGB obtained with the associated standard error. To measure C stock, AGB can be multiplied by a factor of 0.47. In addition, a basic AGB calculation is made using inner-outer diameter, H and ρ.

7 Graphical Representation and Statistical Test

To have a clearer view of the data and the results, graphical representation and statistical tests are needed.

For the DBH, H andρ, their distributions are statistically studied. Boxplots representing the distribution and comparing the 3 species are be made. For DBH and H, frequency, density and Q-Q plots are created. This will help observe the distribution and its potential normality of those distribution. For DBH frequency and density graphs, data with B marked (data recorded at 1 m from the plots edges) samples is also filtered out to compare with the normal data set. This will give an indication on the eventual side effect on the 3 bamboo stands. Normality is assessed on the 3 input variables with the help of Shapiro-Wilk and Lilliefors tests. In addition Kruskal-Wallis and Dunn tests are performed on DBH and H data.

As a graphical representation of the models fitness, fitted AGB values are plotted against observed AGB values and weighted residuals (Huy & Long, 2019).

To asses the fit of the validated models C stocks for adult culms and for young shoots are plotted with their standard error.

8 Softwares

Data were digitized in Microsoft® Excel® for Microsoft 365 MSO (Version 2306 Build 16.0.16529.20164) 64 bits. Modelling and data analysis were made in RStudio Version 2022.07.1 Build 5540.

9 Personnal Contribution

During field trips aimed at measuring parameters, I frequently had the assistance of colleagues to support me in performing these tasks. Laboratory work, including measurements and sample processing, was predominantly carried out by myself, occasionally with the aid of a friend or a faculty member. The sampling plan was devised with input from my supervisors, Professor Meersmans, Professor De Mil, and Nicolas Kovacs. As for the modeling, writing, and layout, I took responsibility for their execution.

III Results

1 Input Parameters: DBH, H and ρ Study

i Diameter at Breast Height

The number of culms DBH measured in each plot was:

- *Phyllostachys Aurea*: 806
- *Phyllostachys Aureosulcata*: 817
- *Phyllostachys Nigra*: 520

A first observation of the DBH distribution can be made in the following graph.

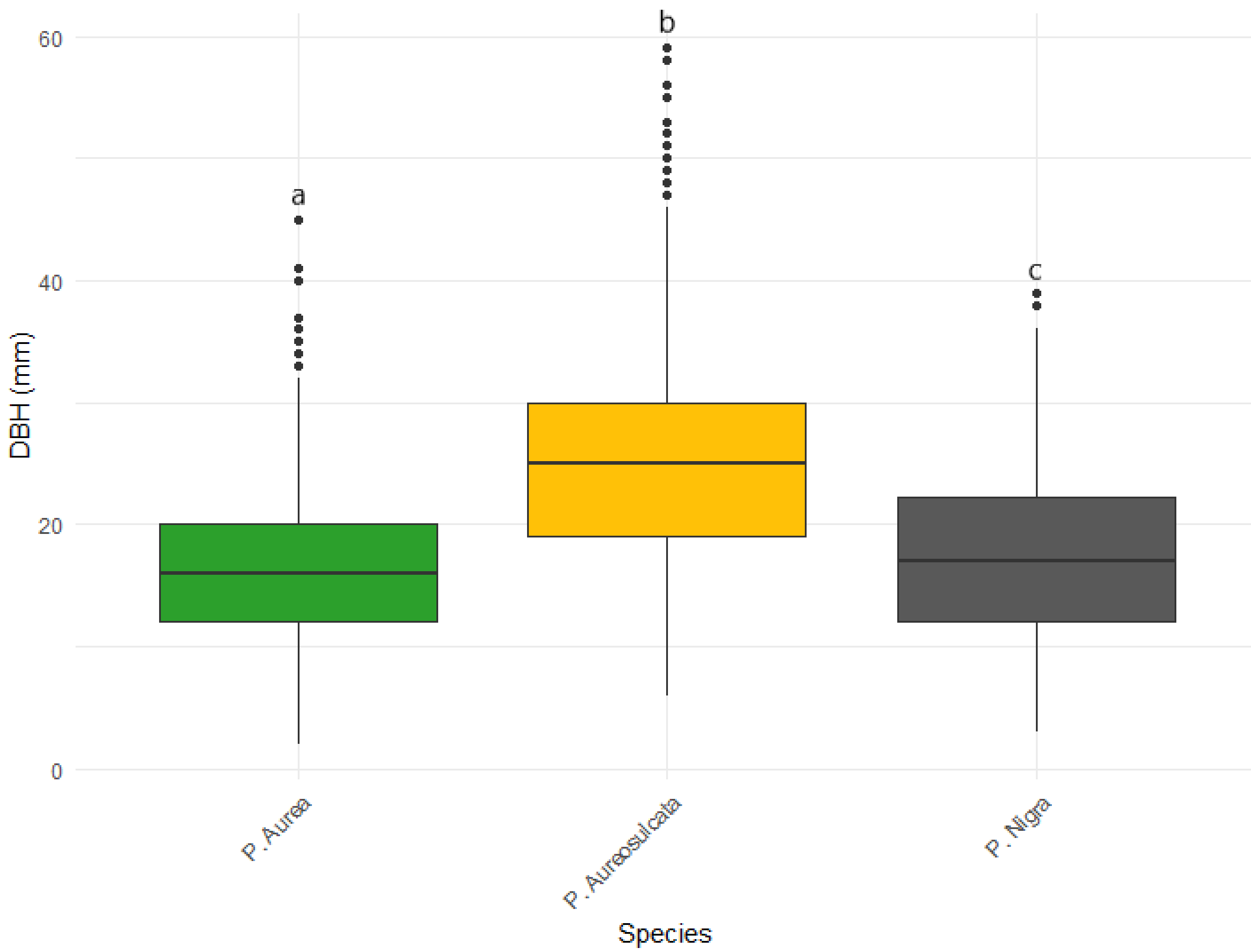

Figure 10: Boxplot representation of the DBH distribution of each species. Different letters indicate significant differences ($p < 0.05$) based on Dunn post-hoc test.

A more thorough investigation made for each species can be found here below.

Phyllostachys Aurea

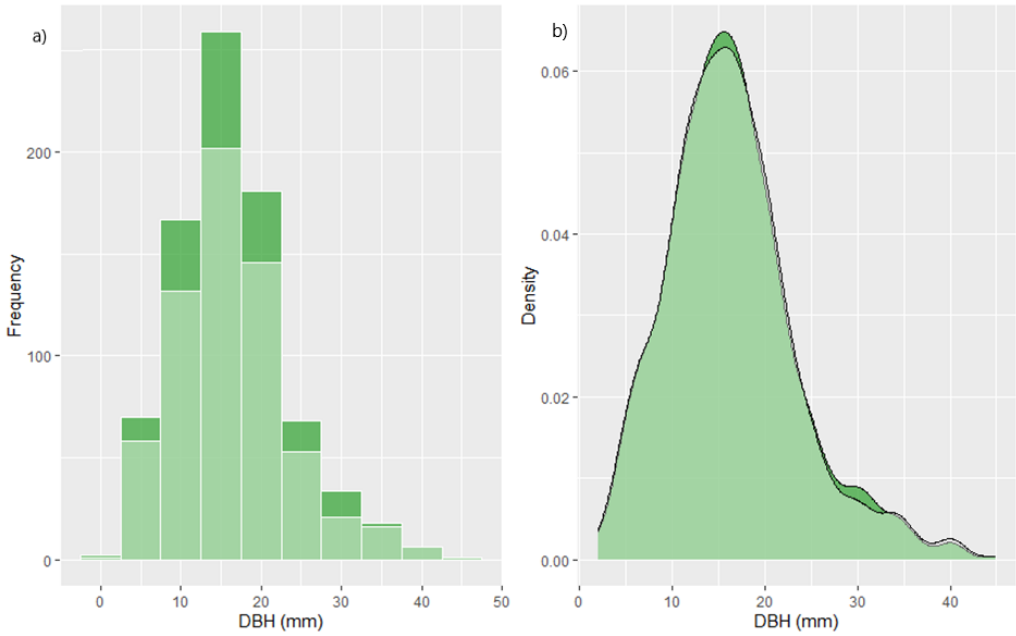

(a) DBH frequency a) and density b) plots of *P. Aurea*. Green data is unfiltered, light green data has side samples (B marked) filtered out, so that the edge effects can be observable.

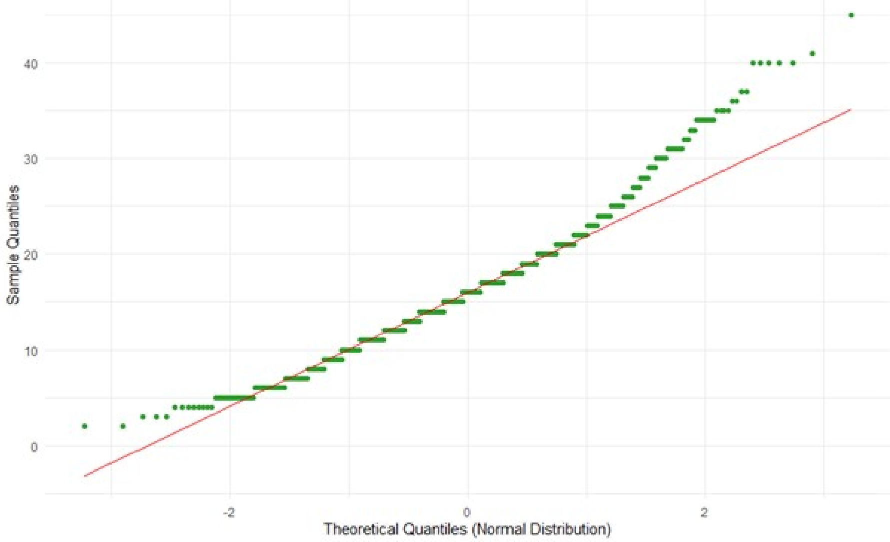

(b) DBH Q-Q plot of *P. Aurea* in order to evaluate the normality of the distribution.

Figure 11: Figures related to *P. Aurea*.

Phyllostachys Aureosulcata

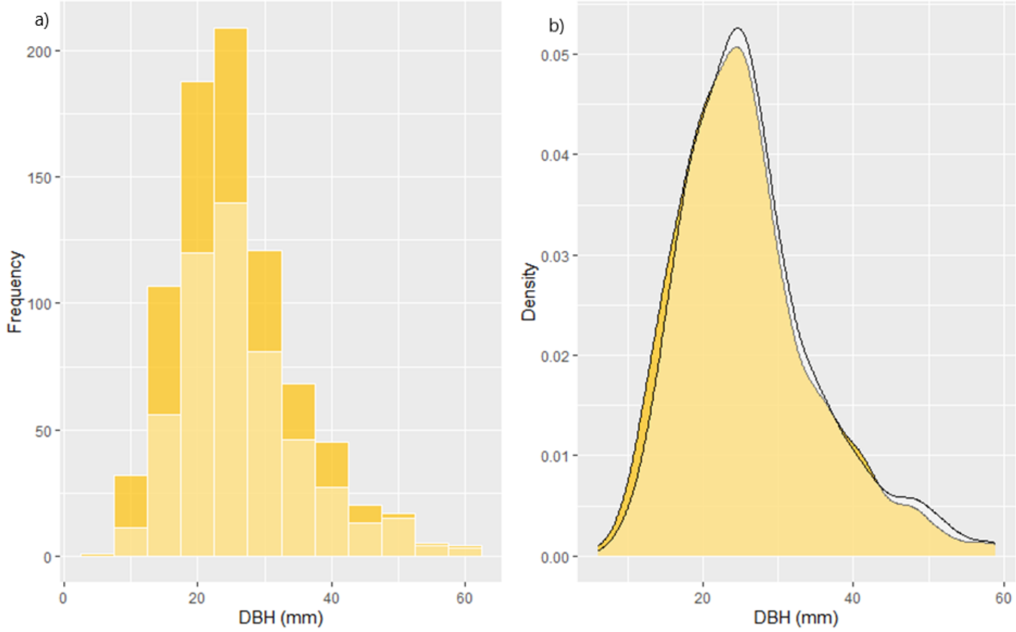

(a) DBH frequency (a) and density (b) plots of *P. Aureosulcata*. Green data is unfiltered, light green data has side samples (B marked) filtered out, so that the edge effects can be observable.

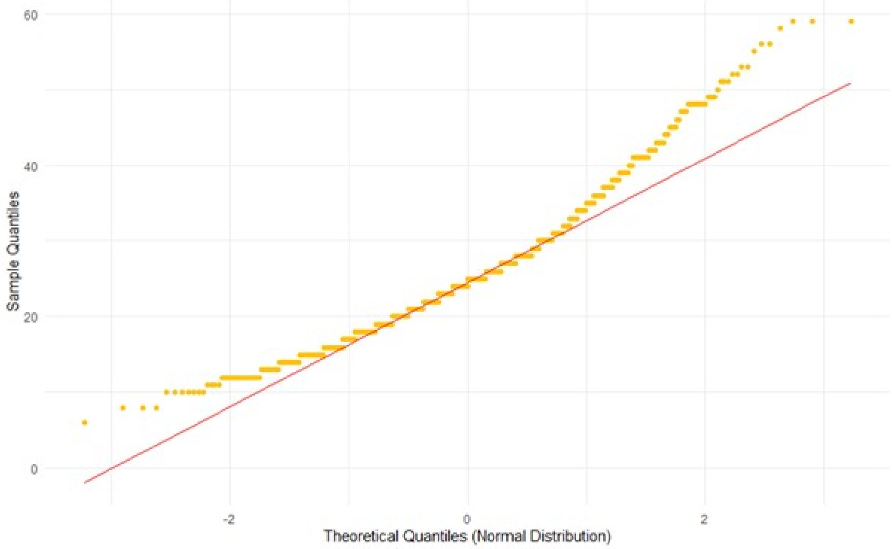

(b) DBH Q-Q plot of *P. Aureosulcata* in order to evaluate the normality of the distribution.

Figure 12: Figures related to *P. Aureosulcata*.

Phyllostachys Nigra

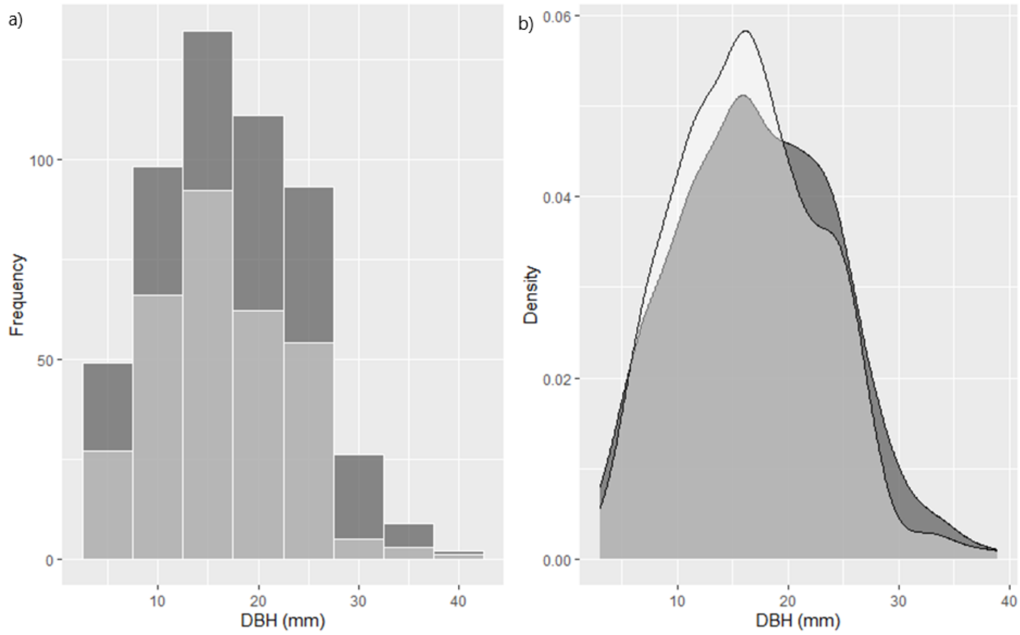

(a) DBH frequency (a) and density (b) plots of *P. Nigra*. Green data is unfiltered, light green data has side samples (B marked) filtered out, so that the edge effects can be observable.

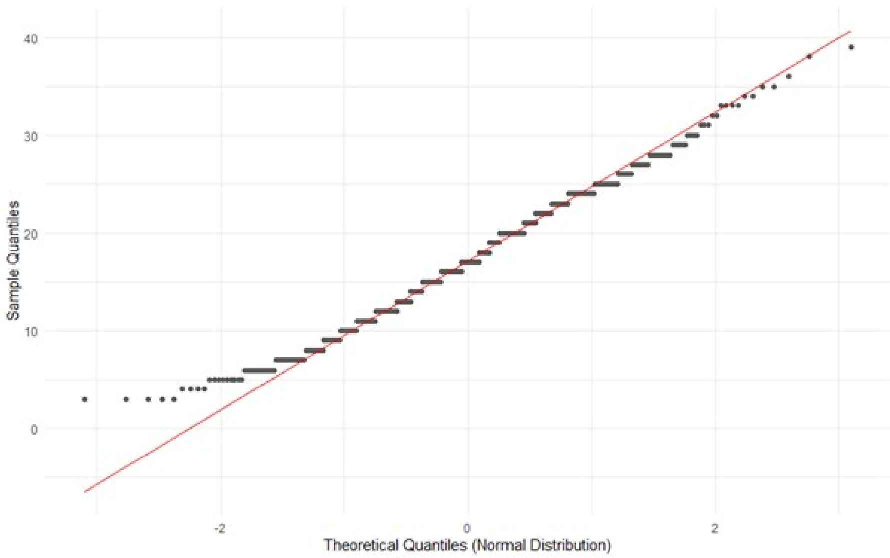

(b) DBH Q-Q plot of *P. Nigra* in order to evaluate the normality of the distribution.

Figure 13: Figures related to *P. Nigra*.

ii Height

The number of culms heights randomly measured in each plot was:

- *Phyllostachys Aurea*: 90
- *Phyllostachys Aureosulcata*: 90
- *Phyllostachys Nigra*: 60

These numbers represents approximately 10% of the culms in each of the plots. A first observation of the H distribution can be made with the following figures (Figures 14 and 15).

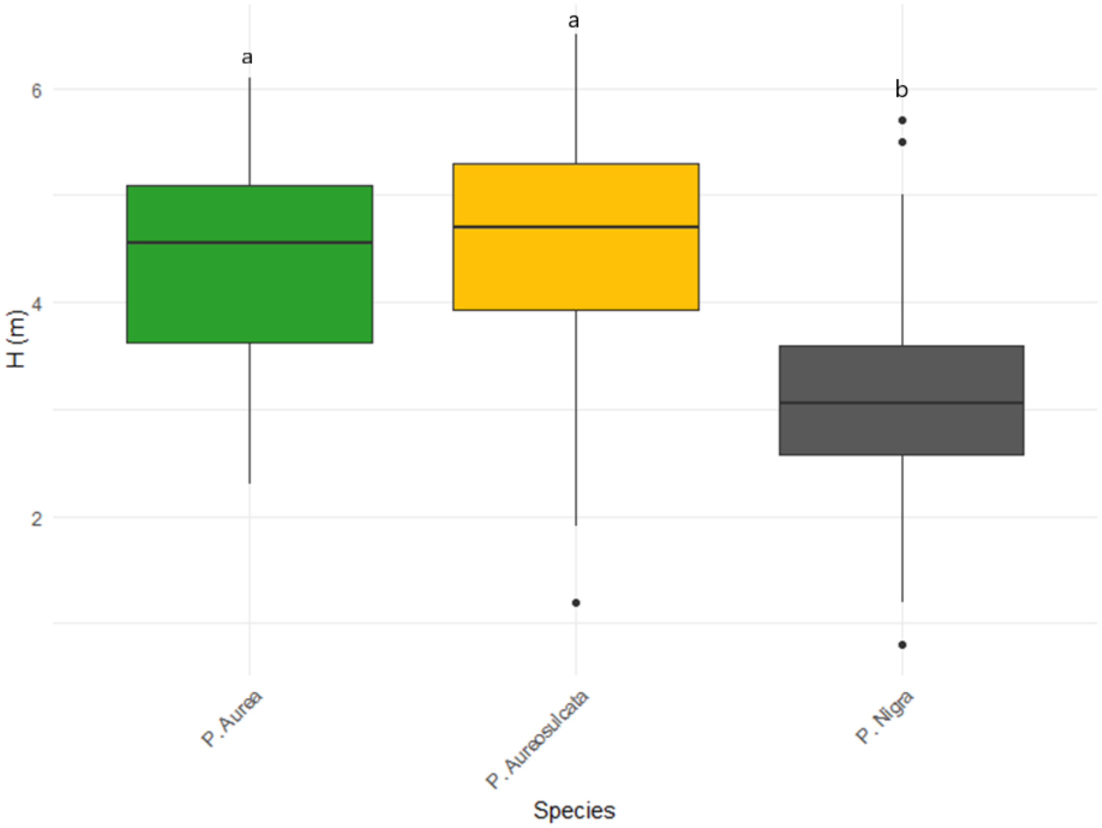

Figure 14: Boxplot representation of the H distribution of each species. Different letters indicate significant differences ($p < 0.05$) based on Dunn post-hoc test.

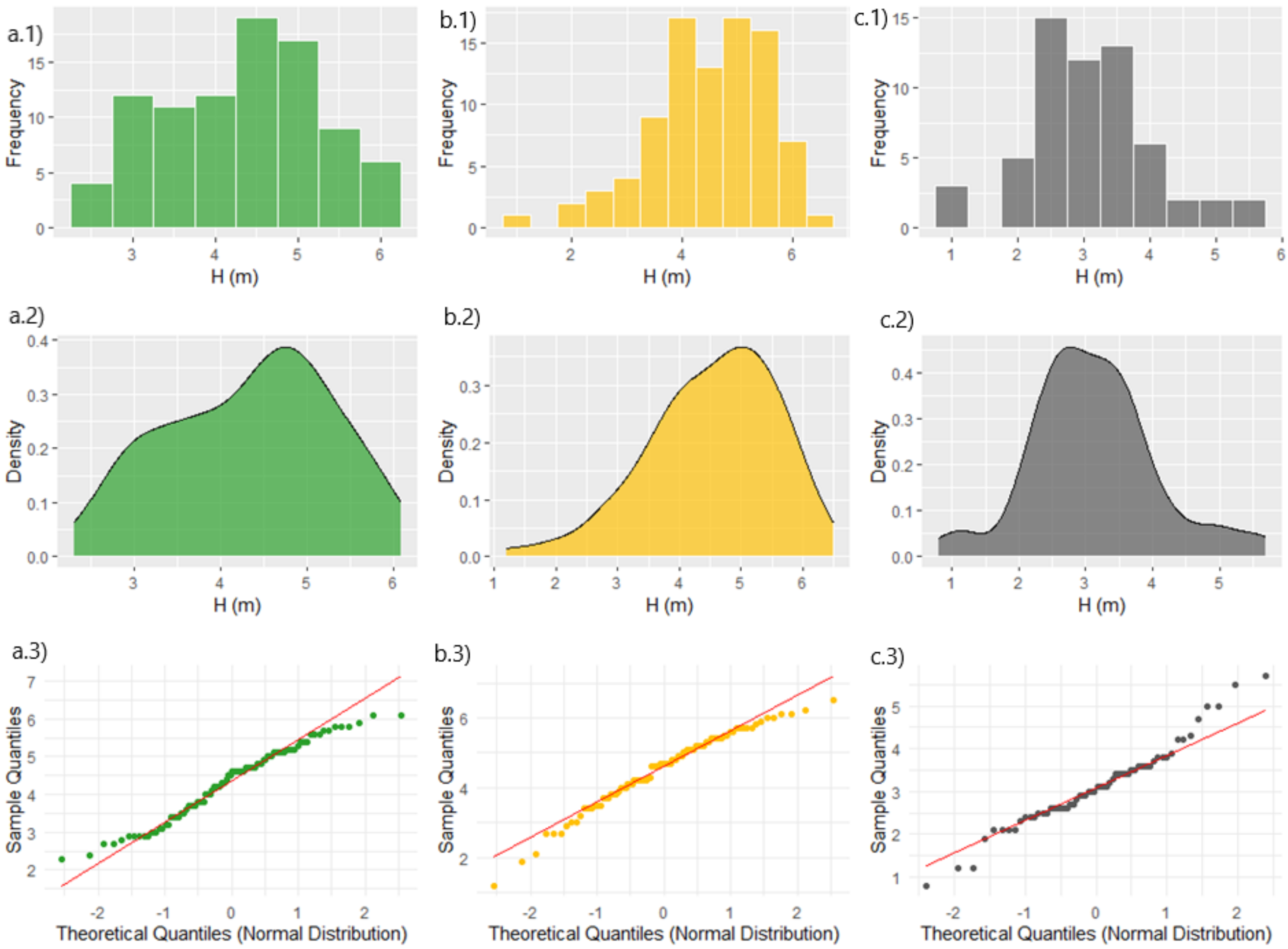

Figure 15: Height frequency distribution (1), density ditsibution (2) and QQ-plots (3) of *P.Aurea* (a), *P.Aureosulcata* (b) and *P.Nigra* (c).

iii Basic Density

The number of culms basic densities measured in total was:

- *Phyllostachys Aurea*: 10
- *Phyllostachys Aureosulcata*: 9
- *Phyllostachys Nigra*: 10

This represents the total sampled and analyzed in laboratory culms (except for 1 error in P.Aureosulcata).

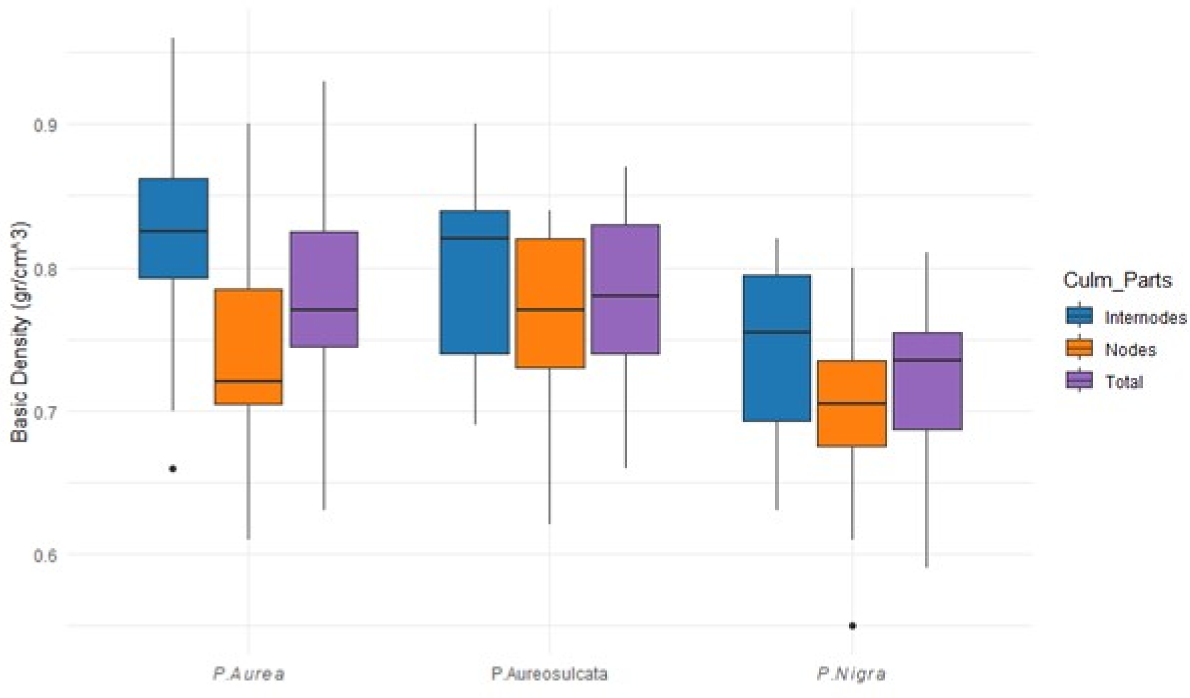

Figure 16: Boxplot representation of culm parts basics densities and their total (mean) for each species.

iv Resume Table

To conclude this section, a resume is available : Table 2.

Table 2: DBH, H, and ρ resume for the 4 groups with number of measurements, Minimum value, Maximum Value, Mean value and standard deviation. P-values of normality tests from Shapiro-Wilk and Lilliefors for DBH and H of the 3 species.

Species	Parameter	Data (N)	Min	Max	Mean	Standard Deviation	Shapiro-Wilk p-value	Lilliefors p-value
Multi-Species	DBH (mm)	2143	2.00	59.00	20.15	9.02		
	H (m)	240	0.80	6.50	4.10	1.17		
	ρ Node (gr*cm^{-3})	29	0.55	0.90	0.73	0.08		
	ρ Internode (gr*cm^{-3})	29	0.63	0.96	0.78	0.08		
	ρ (gr*cm^{-3})	29	0.59	0.93	0.76	0.08		
P.Aurea	DBH	806	2.00	45.00	16.42	6.97	<0.001	<0.001
	H	90	2.30	6.10	4.34	0.96	<0.05	<0.05
	ρ Node	10	0.61	0.90	0.74	0.08		
	ρ Internode	10	0.66	0.96	0.82	0.09		
	ρ	10	0.63	0.93	0.78	0.08		
P.Aureosulcata	DBH	817	6.00	59.00	25.68	9.18	<0.001	<0.001
	H	90	1.20	6.50	4.54	1.05	<0.05	<0.05
	ρ Node	9	0.62	0.84	0.76	0.07		
	ρ Internode	9	0.69	0.90	0.80	0.07		
	ρ	9	0.66	0.87	0.78	0.07		
P.Nigra	DBH	520	3.00	39.00	17.25	7.02	<0.001	<0.001
	H	60	0.80	5.70	3.12	0.98	>0.1	>0.1
	ρ Node	10	0.55	0.80	0.70	0.07		
	ρ Internode	10	0.63	0.82	0.74	0.07		
	ρ	10	0.59	0.81	0.72	0.07		

2 Modelling

A long list of models was tested. The combinations of 2 different regression (linear and nonlinear regression), mixed input variables and different weightings were tested. The full list of tests can be found in Appendix C. Only the selected models that passed cross-validation will be presented in this section (Table 3).

i Overview of selected models

Multi-Species .

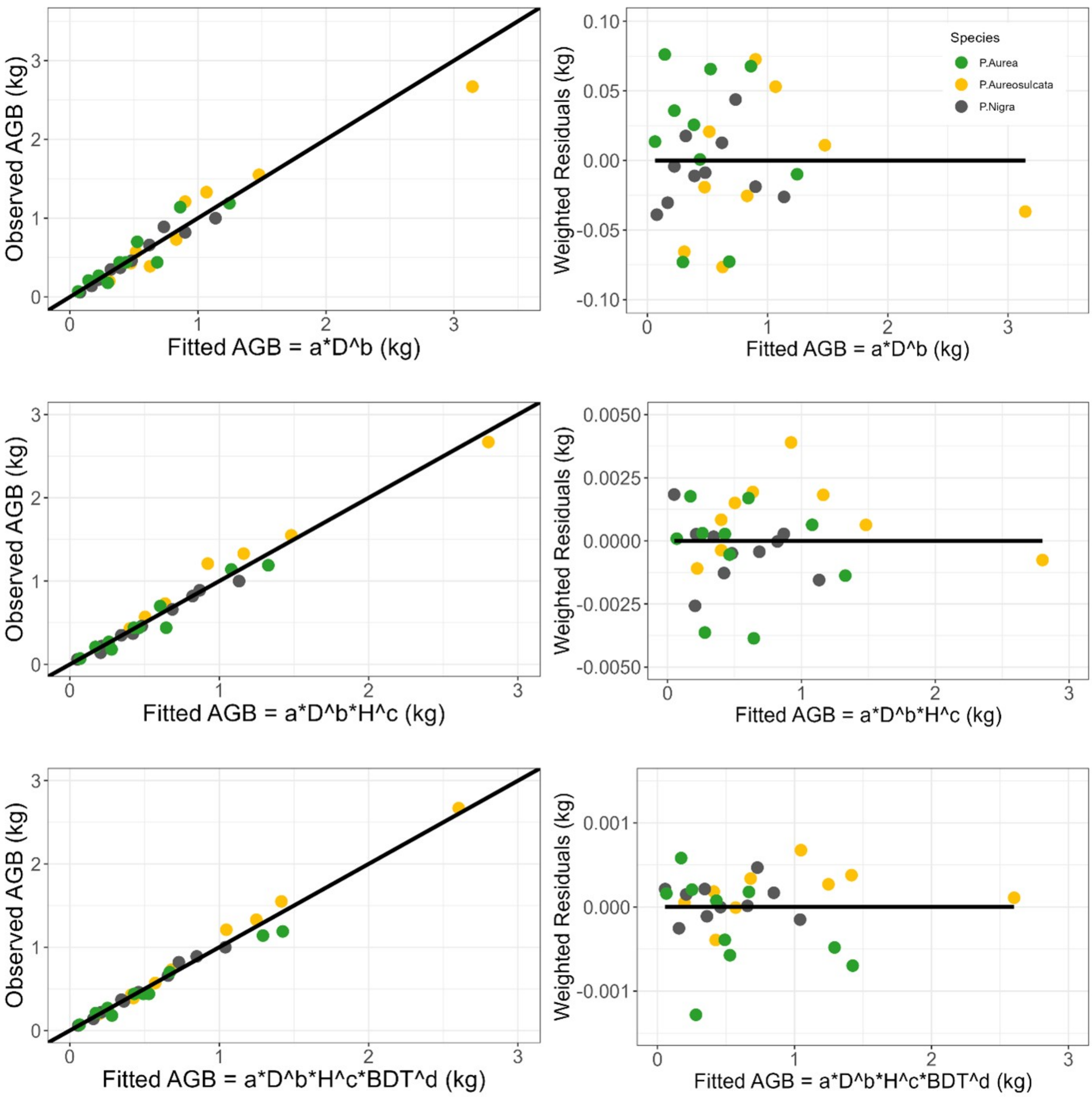

Figure 17: Resume of fitted AGB In relation with observed AGB and weighted residuals of multi-species models(*M1, M2, M3*).

Table 3: Resume of selected models with reference ID, formulas and performance parameters

ID	Formula	R2 (-)	R2adj (-)	AIC (-)	Bias (%)	RMSE (kg)	MAPE (%)
	Muli-Species						
M1	AGB = 0.1756 $\times D^{1.7838}$	0.917	0.907	-33.711	-5.619	0.158	19.966
M2	AGB = 0.0467 $\times D^{1.1511} \times H^{1.0864}$	0.970	0.966	-49.034	-2.786	0.094	12.418
M3	AGB = 0.0702 $\times D^{1.1820} \times H^{0.9940} \times \rho^{1.0356}$	0.980	0.976	-56.141	-1.290	0.078	9.098
	P.Aurea						
A1	log(AGB) = -5.4705 + 2.9284 $\times log(H)$	0.982	0.973	-27.624	-0.511	0.050	7.159
A2	AGB = 0.0042 $\times H^{2.9337}$	0.981	0.972	-27.495	-0.678	0.050	7.158
A3	AGB = 0.0016 $\times D^{-0.4704} \times H^{3.6827}$	0.956	0.920	-23.879	0.453	0.078	6.991
	P.Aureosulcata						
AS1	log(AGB) = -4.1244 + 2.4181 $\times log(H)$	0.954	0.926	-3.700	-1.961	0.157	13.753
AS2	AGB = 0.0166 $\times H^{2.4078}$	0.953	0.926	0.984	-2.209	0.158	13.855
	P.Nigra						
N1	log(AGB) = -3.8910 + 1.9534 $\times log(H)$	0.798	0.697	-6.910	-7.211	0.140	24.913
N2	AGB = 0.1527 $\times D^{2.0874}$	0.811	0.716	-24.650	-5.427	0.136	10.945
N3	AGB = 0.0056 $\times H^{2.8133}$	0.912	0.868	-6.591	-2.456	0.093	24.494
N4	AGB = 0.0929 $\times D^{1.5459} \times H^{0.4758}$	0.967	0.940	-23.226	-1.373	0.057	7.834

P.Aurea .

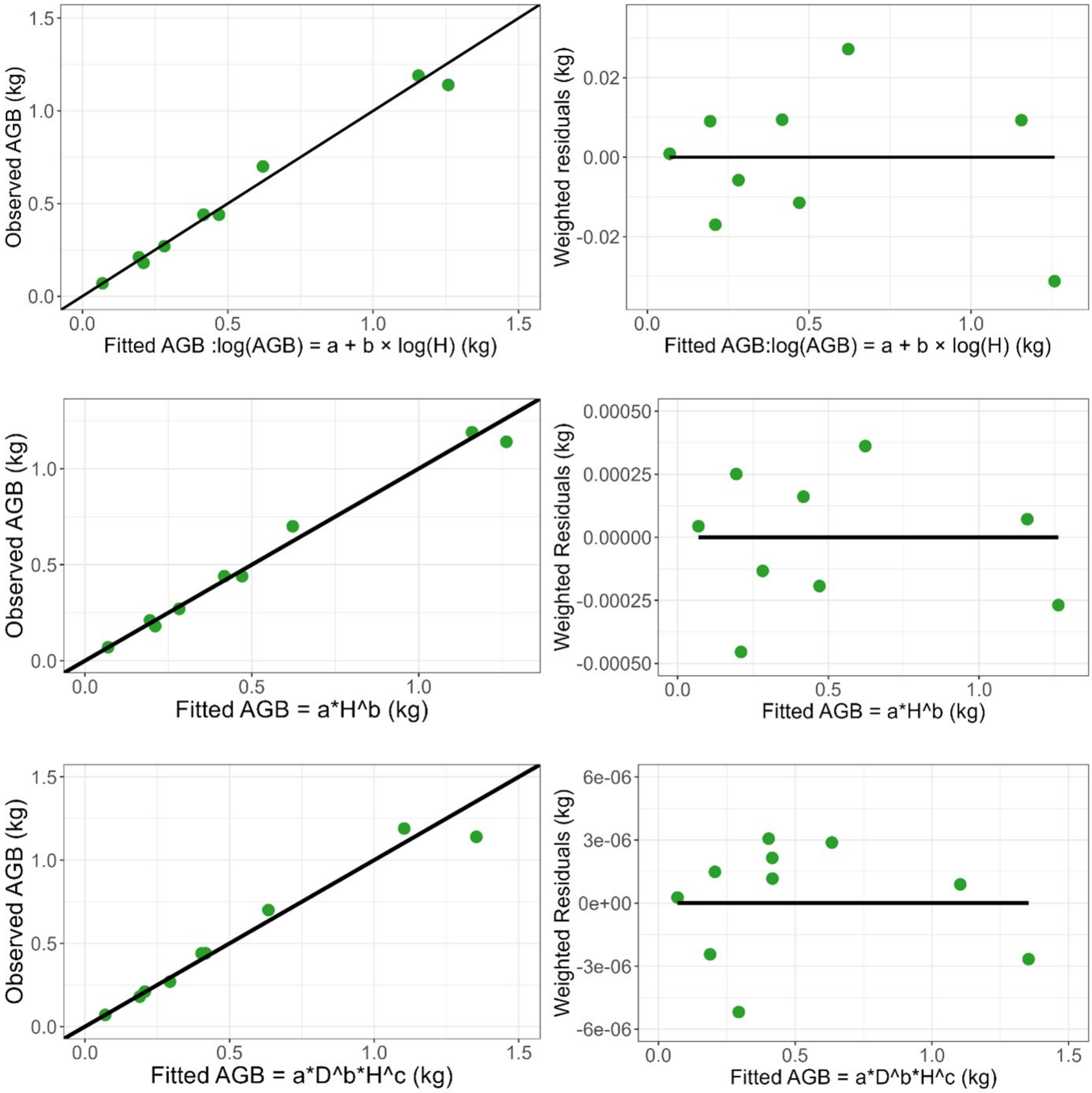

Figure 18: Resume of fitted AGB In relation with observed AGB and weighted residuals of *P.Aurea* models(*A1, A2, A3*).

P.Aureosulcata .

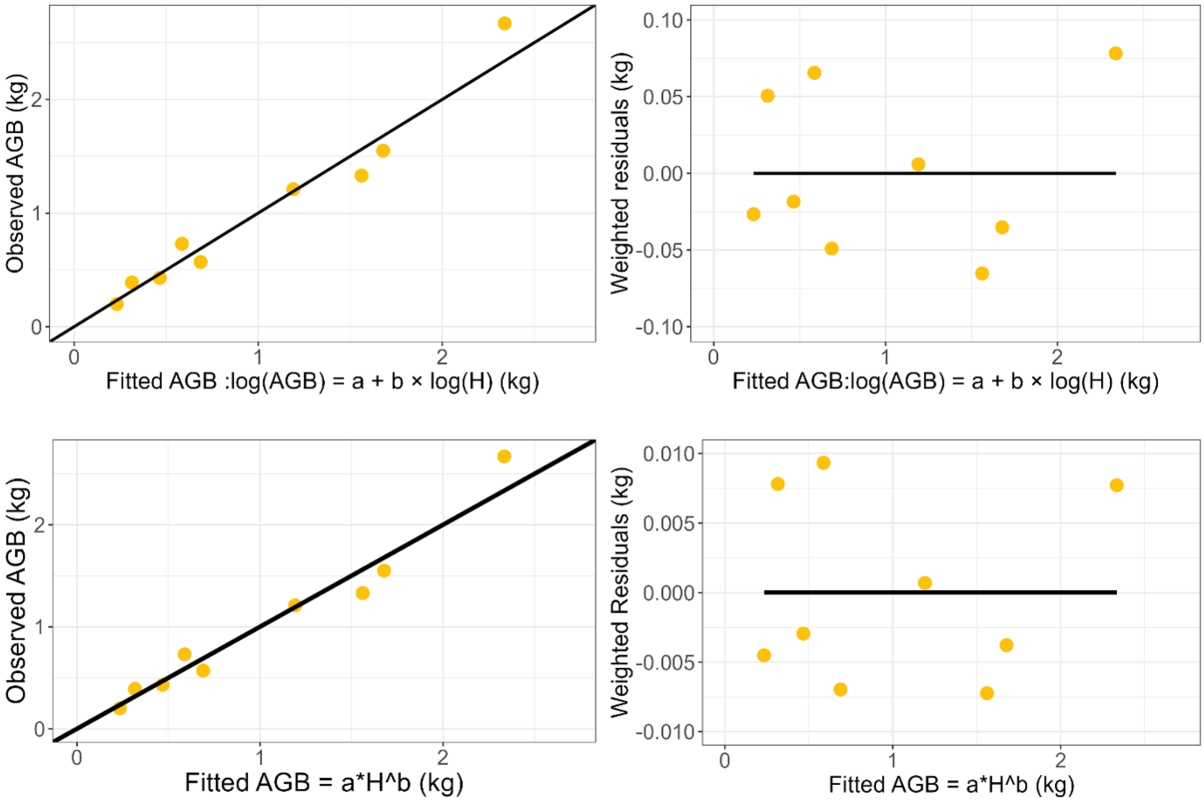

Figure 19: Resume of fitted AGB In relation with observed AGB and weighted residuals of *P.Aureosulcata* models(*AS1*, *AS2*).

P.Nigra .

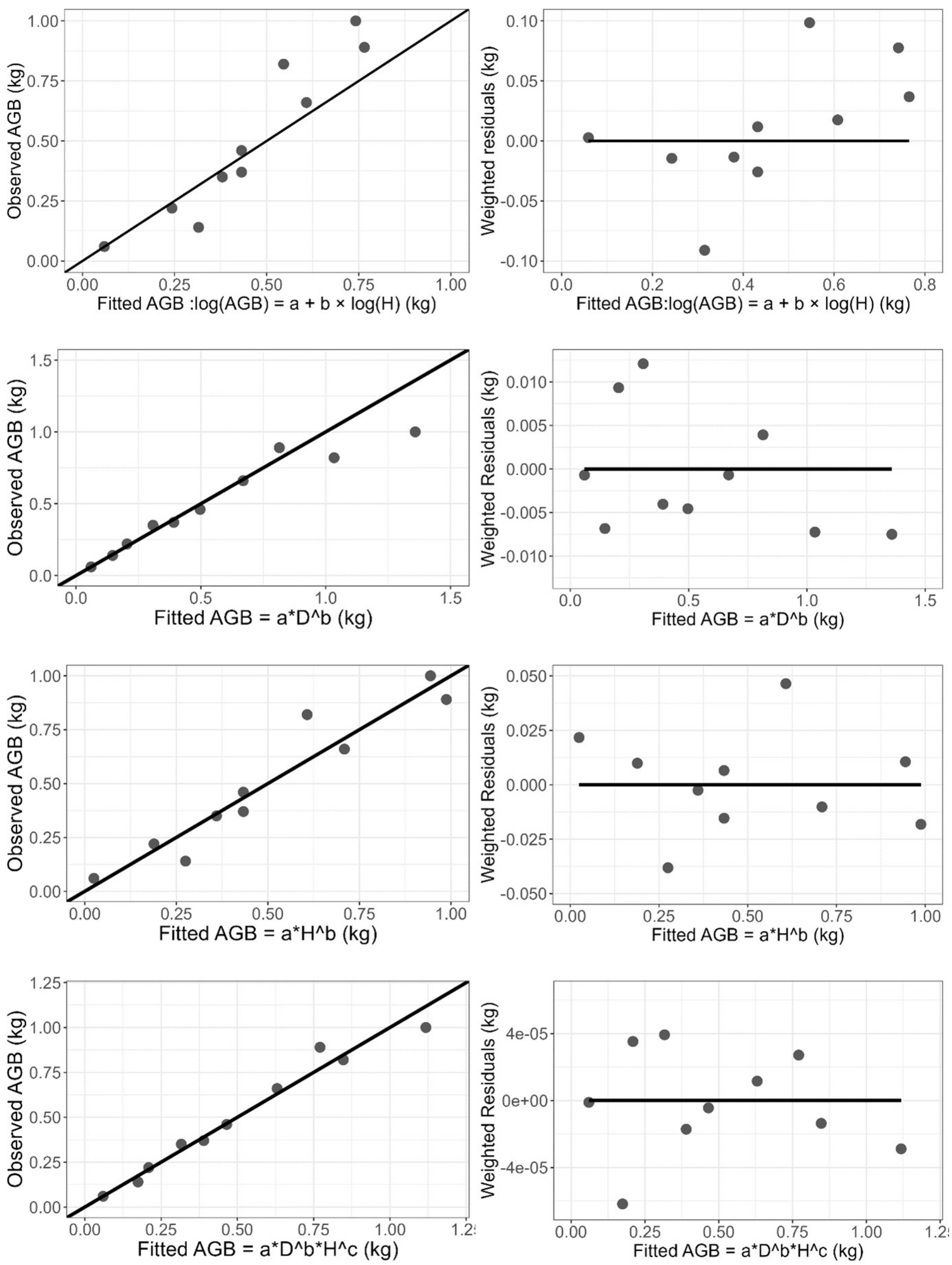

Figure 20: Resume of fitted AGB In relation with observed AGB and weighted residuals of *P.Nigra* models(*N1, N2, N3, N4*).

Relation between Aboveground Biomass, DBH and H .

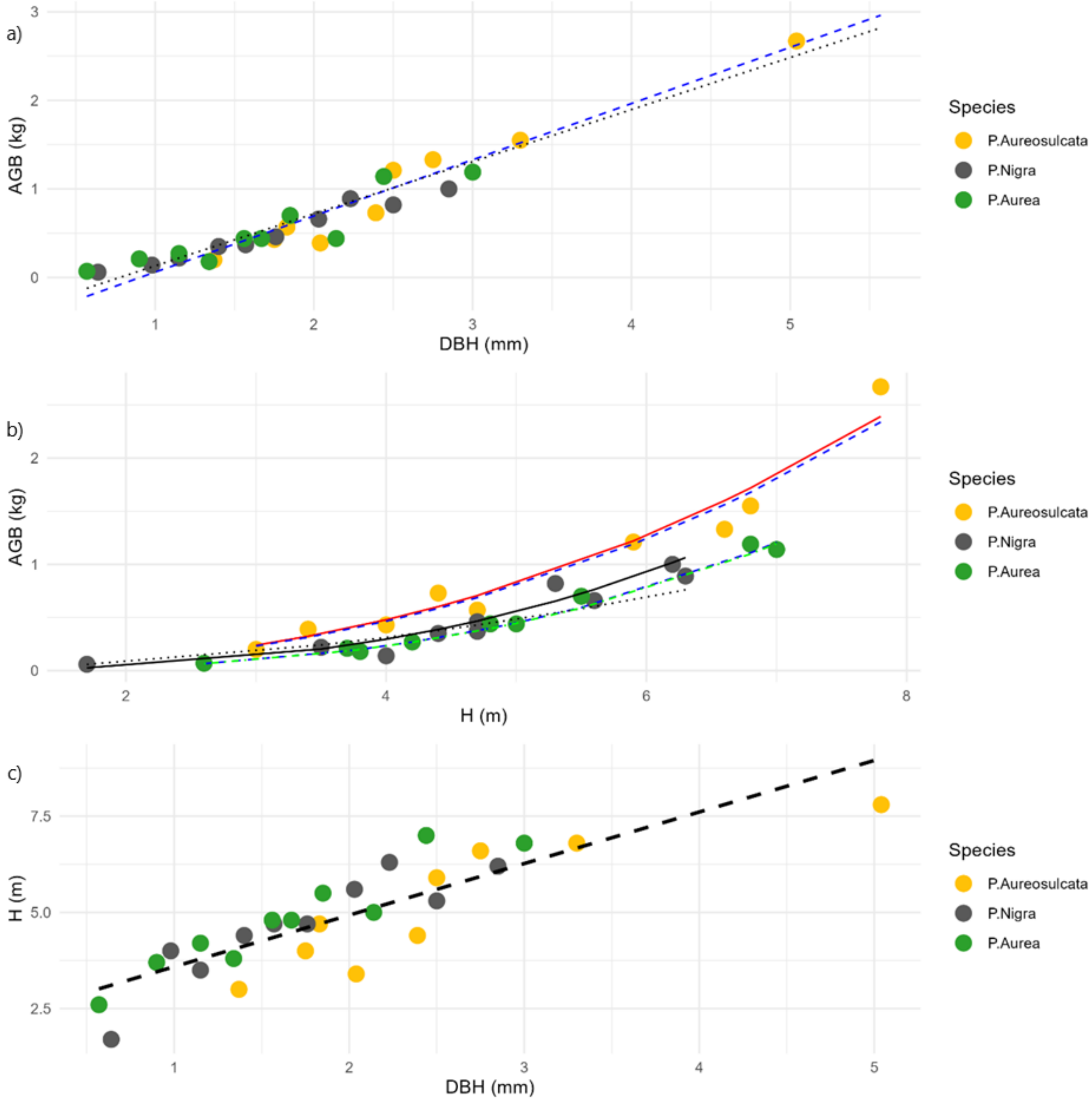

Figure 21: Relation between DBH, H and basic models (with one parameter): above (a) doted-black line: *N2* ; dashed-blue line : *M1* ; middle (b) solid-black line: *N3* ; solid-red line : *AS2* ; dashed-blue line: *A2* ; doted-black line : *N1* ; dashed-blue line : *AS1* ; dotdashed-green line: *A1* ; bottom(c) dashed-black line, correlation line between D an H (correlation = 0.86). Model References are from Table 3.

With those 12 selected models (Table 3), it is now possible to estimate Aboveground Biomass and also Carbon stock.

3 Above ground Biomass and Carbon Stocks estimations

One key component to estimate AGB on larger scales, is culm density, it can be found in Table 4.

Table 4: Culm density of the adult culms of the 4 groups, based on plot area and the number of culms.

Species	Plot Area (m^2)	Nbr of culms	Culm density (culms * m^{-2})
Multi-species	349.75	2143.00	6.13
P.Aurea	57.15	806.00	14.10
P.Aureosulcata	199.54	817.00	4.09
P.Nigra	93.06	520.00	5.59

With the use of a volume formula, AGB and Carbon Stocks can be calculated. Those results can be found in Table 5.

Table 5: Mathematicaly estimated AGB and C stocks for the 4 groups. Estimation trough the use of volume. Total is culm multiplied by an estimated factor of 1.3 to account for the culm percentage in the total biomass, as roughly approximated out of Nath and Das, 2011; Yen, 2016. Mean AGB represent the mean estimation by culm. AGBT represent the estimated total AGB on each plot at Merksplas. AGB is the estimated Aboveground Biomass in *Ton* by *ha* and C is the estimated Carbon Stock in *Ton* by *ha*.

Species	Part	Mean AGB (kg)	AGBT (kg)	AGB(Ton * ha^{-1})	C(Ton * ha^{-1}))
Multi-species	Culm	0.43	932.04	26.66	12.53
	Total	0.57	1211.65	34.66	16.29
P.Aurea	Culm	0.40	319.64	55.92	26.28
	Total	0.52	415.53	72.69	34.17
P.Aureosulcata	Culm	0.71	583.38	29.20	13.73
	Total	0.93	758.39	37.97	17.84
P.Nigra	Culm	0.25	129.31	13.90	6.53
	Total	0.32	168.11	18.07	8.49

The next step is the estimation trough the use of the selected models in Table 3. The results can be found in the next Table 6.

Table 6: Estimated AGB and C stocks with the help of selected models (see Table 3 for the 4 groups. Mean AGB represent the mean estimation by culm. AGBT represent the estimated total AGB on each plot at Merksplas. AGB is the estimated Aboveground Biomass in *Ton* by *ha* and C is the estimated Carbon Stock in *Ton* by *ha*.

Multi-species	MeanAGB(kg)	AGBTotal(kg)	AGB(kg*m^{-2})	AGB(Ton*ha^{-1})	C(Ton*ha^{-1})
M1	0.671 ± 0.011	1439.50 ± 25.12	4.115 ± 0.072	41.12 ± 0.72	19.33 ± 0.34
M2	0.508 ± 0.021	1088.30 ± 45.69	3.114 ± 0.131	31.14 ± 1.31	14.64 ± 0.62
M3	0.509 ± 0.020	1091.42 ± 42.78	3.123 ± 0.123	31.21 ± 1.23	14.67 ± 0.58
P.Aurea					
A1	0.346 ± 0.020	278.95 ± 16.48	4.881 ± 0.288	48.81 ± 2.88	22.94 ± 1.36
A2	0.286 ± 0.019	230.50 ± 15.37	4.033 ± 0.269	40.33 ± 2.69	18.96 ± 1.26
A3	0.371 ± 0.031	299.26 ± 24.37	5.236 ± 0.426	52.36 ± 4.26	24.61± 2.00
P.Aureosulcata					
AS1	0.684 ± 0.034	558.97 ± 27.83	2.801 ± 0.139	28.01 ± 1.39	13.17 ± 0.66
AS2	0.622 ± 0.033	507.98 ± 26.63	2.546 ± 0.133	25.46 ± 1.33	11.96 ± 0.63
P.Nigra					
N1	0.203 ± 0.017	105.53 ± 8.81	1.134 ± 0.095	11.34 ± 0.95	5.33 ± 0.45
N2	0.578 ± 0.022	300.38 ± 10.17	3.228 ± 0.109	32.27 ± 1.09	15.17 ± 0.51
N3	0.170 ± 0.021	88.20 ± 11.12	0.948 ± 0.119	9.48 ± 1.19	4.45 ± 0.56
N4	0.376 ± 0.010	195.61 ± 5.36	2.102 ± 0.058	21.01 ± 0.58	9.88 ± 0.27

4 Potential Carbon sink measurement

In this part, a part of the C sink will be estimated with the measurement of young culms i.e. this year new shoots. A first look at the DBH and H data of young culms can be done in Table 7.

Table 7: Number of young shoots measured at the beginning of July, with DBH and H mean and standard deviation. The young shoots culm density is also calculated.

		H (m)	DBH (mm)	Nculms	Culm density (culms * m^2)
Multi-species	Mean	2.89	20.65	237	0.68
	SD	1.82	9.62		
P.Aurea	Mean	2.23	20.14	46	0.80
	SD	1.89	7.8		
P.Aureosulcata	Mean	3.01	24.98	87	0.44
	SD	2.32	11.59		
P.Nigra	Mean	3.08	17.25	104	1.12
	SD	1.15	6.77		

With this new data, it is possible to estimate the potential C sink from the new shoots (Table 8).

Table 8: Estimated AGB and C stocks with the help of selected models (see Table 3) for the 4 groups of young shoots. Mean AGB represent the mean estimation by culm. AGBT represent the estimated total AGB on each plot at Merksplas. AGB is the estimated Aboveground Biomass in *Ton* by *ha* and C is the estimated Carbon Stock in *Ton* by *ha*. Model references (*m1, m2,...*) are on the left column.

Multi-species	Mean AGB(kg)	AGBTotal(kg)	AGB(kg*m^{-2})	AGB(Ton*ha^{-1})	AGC(Ton*ha^{-1})
m1	0.74 ± 0.04	174.5 ± 9.4	0.50 ± 0.03	4.99 ± 0.27	2.34 ± 0.13
m2	0.37 ± 0.02	87.8 ± 4.9	0.25 ± 0.01	2.51 ± 0.14	1.18 ± 0.07
m3	0.37 ± 0.02	88.6 ± 5.2	0.25 ± 0.01	2.53 ± 0.15	1.19 ± 0.07
P.Aurea					
a1	0.13 ± 0.03	6.2 ± 1.4	0.11 ± 0.02	1.08 ± 0.25	0.51 ± 0.12
a2	0.18 ± 0.04	8.2 ± 1.6	0.14 ± 0.03	1.43 ± 0.29	0.67 ± 0.14
a3	0.14 ± 0.03	6.4 ± 1.6	0.11 ± 0.03	1.12 ± 0.28	0.52 ± 0.13
P.Aureosulcata					
as1	0.47 ± 0.07	40.9 ± 5.7	0.20 ± 0.03	2.05 ± 0.29	0.96 ± 0.13
as2	0.28 ± 0.05	24.1 ± 4.9	0.12 ± 0.02	1.21 ± 0.24	0.57 ± 0.11
P.Nigra					
n1	0.21 ± 0.01	21.6 ± 1.2	0.23 ± 0.01	2.32 ± 0.13	1.09 ± 0.06
n2	0.56 ± 0.04	58.4 ± 4.3	0.63 ± 0.05	6.28 ± 0.46	2.96 ± 0.21
n3	0.18 ± 0.01	18.5 ± 1.4	0.20 ± 0.01	1.99 ± 0.15	0.93 ± 0.07
n4	0.38 ± 0.02	38.2 ± 2.4	0.41 ± 0.03	4.10 ± 0.26	1.93 ± 0.12

5 Comparison of Carbon stock and Carbon sink

The estimated C stock and C sink (in *Ton* by *ha*) are now known thanks to the use of the previously selected models. We can now also visually compare the estimated C stock (Figure 22) and C sink (Figure 23).

6 Other results

Regarding the pH measurements, it was observed thet the 3 plots have a pH of approximatively 5.

Regarding the leave nets, due to multiple issues (broken nets, not enough measurements data, no possibility to observe the leaves nets multiple seasons like Devi and Singh, 2021 did for exemple) the results will not be displayed in this study, however the raw data can be found in Appendix D.

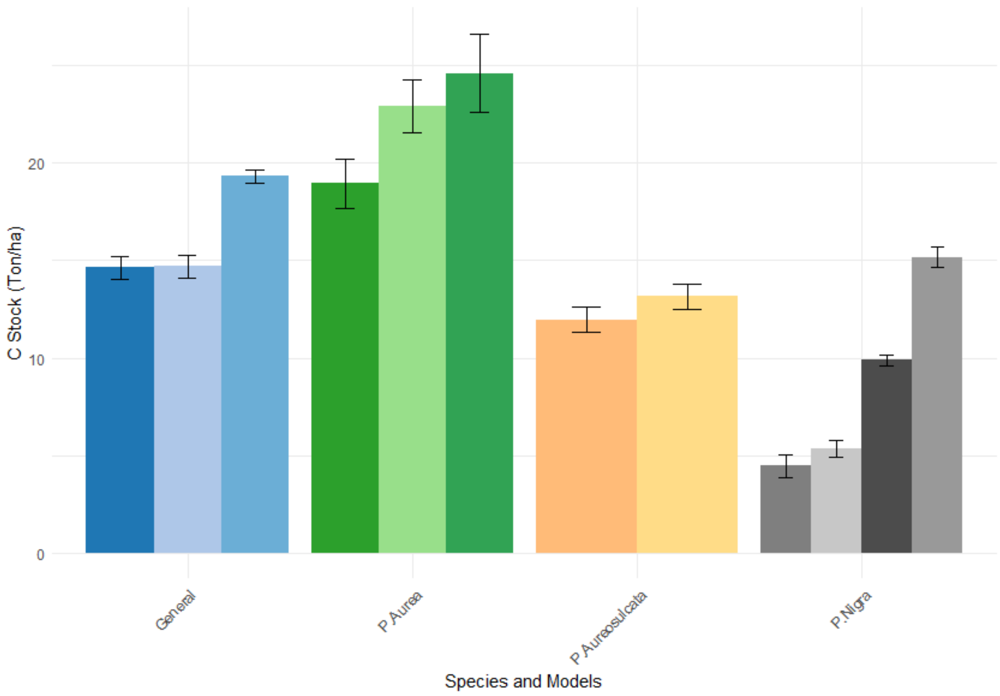

Figure 22: Estimation of the C stock (in *Ton* by *ha*) by the selected models in rising order by group i.e. for general (Multi-species) : *M2, M3, M1*; for *P.Aurea* : *A2, A1, A3* ; for *P.Aureosulcata* : *AS2, AS1*; and for *P.Nigra* : *N3, N1, N4, N2.*

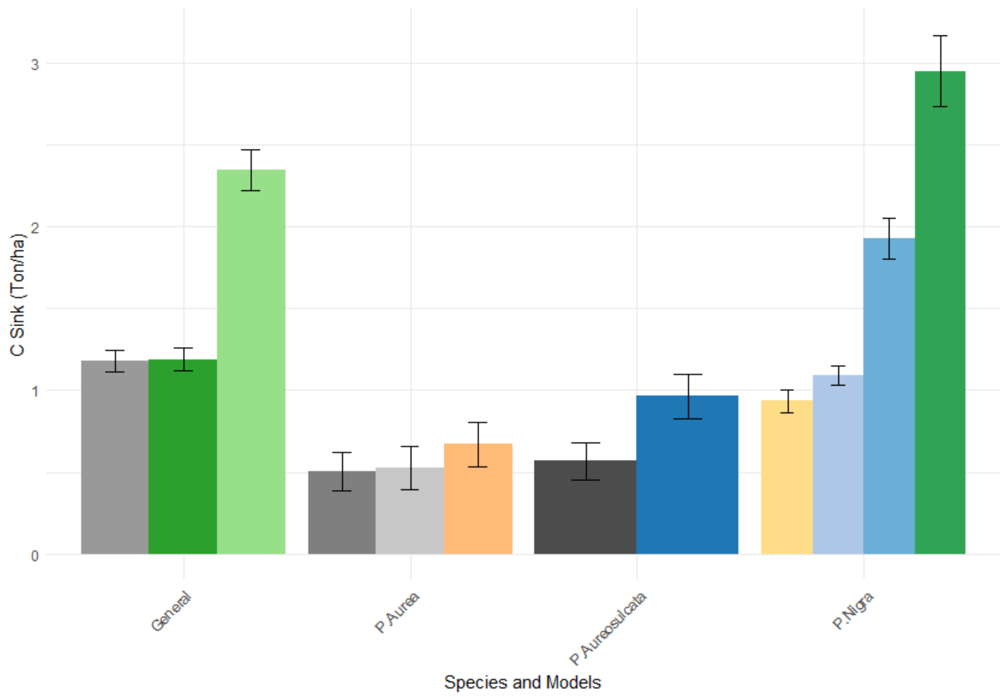

Figure 23: Estimation of the C stock (in *Ton* by *ha*) by the selected models in rising order by group i.e. for general (Multi-species) : *M2, M3, M1*; for *P.Aurea* : *A1, A3, A2* ; for *P.Aureosulcata* : *AS2, AS1*; and for *P.Nigra* : *N3, N1, N4, N2.*

IV Discussion

1 DBH, H and ρ distributions

i Diameter at Breast Height

The DBH study of the three *Phyllostachys* species returned smaller values (Table 2) than what is described in the literature (Liese, 1985 cited by Liese and Köhl, 2015;*Phyllostachys aureosulcata* McClure, J. Wash. Acad. Sci. 35: 282. 1945, cited by "Flora of China: Bambusoideae", n.d.). This can be due to various factors like the age of the plantation, the management practices, the site (location, elevation, etc), and climatic conditions (Cao et al., 2019; Liese & Köhl, 2015; Xu et al., 2018). In newly established bamboo stands, DBH varies with the age, and it tends to keep growing with time (Kuehl et al., 2013). In this study case, bamboo stands can be considered as young. This is even more true for the *P.Nigra* stand, the plot was destroyed 3 years ago because of harsh climatic conditions. In consequence, all remaining culms were cut down. In addition, due to management practices, for the 3 plots the 3 year old culms are usually taken out. To take into account edge effects (with edges of the plantation being most exposed to sunlight), a quick analysis of the DBH distribution with and without the B marked data. It showed no major differences (Figure 11a,12a,13a). Thus, the investigation regarding an eventual edge effect was not pursued.

Altought the density and frequency plot (Figures 11a,12a,13a) showed no clear sign of an anormal distribution, he observation of the QQ-plots (Figures 11b, 12b, 13b) indicated the possibility that the DBH distributions were not normal. The normality tests (Table 2) for the three species each rejected the hypothesis that the DBH distribution was normal. This can be explained by the fact that those plots are under management, so they don't represent a natural distribution. In the case of managed bamboo stands, usually, a part of older culms is being collected each year. This lowers the representation of older (so, often larger) culms in comparison to younger culms. However, this isn't an issue because studies regarding bamboo AGB usually take place in managed plantations. The Kruskal-Willis test showed that at least one species was different from the others in terms of DBH. The following Dunn test indicated that every species was different from the two other species.

ii Height

Similar to the DBH, the heights study showed smaller values compared to the ones found in the literature. The same factors than for DBH can be advanced to explain this variation. The observation of the 3 different plots (Figure 15) can suggest that the distribution is not normal. Indeed, the different normality tests (Table 2) confirmed that suggestion, except for *P.Nigra*. Further investigation with the Kruskal-Wallis and Dun tests showed that *P.Nigra* heights can be considered different than the two others, however heights from *P.Aurea* and *P.Aureosulcata* are not significantly different. Even if the H data reported here looks lower than in the literature, the comparison between the three species looks similar. In both, *P.Nigra* H seems different and smaller than the two other species. This could be an indication of the afore described factors effects on the heights. However, this is just a hypothesis, and it needs further investigation to be proven. Also, it is important to recall that the culms on the *P.Nigra* plot are a bit younger than those on the other plots.

iii Basic Density

Basic density of the 3 species (Figure 16) were higher than what can be found in other studies. For *P.Aurea*, a basic density of 0.77+-0.08 $gr*cm^{-3}$ was measured. It is higher than values of 0.647; 0.48+-0.03 and 0.53 that can be found respectively in Rusch et al., 2021, Sette Júnior et al., 2017, and Mbamu et al., 2020. *P.Aureosulcata* basic density was measured at 0.78+-0.07 but it proven itself difficult to find values from this specific species to compare with. Values measured for *P.Nigra* were 0.72 +- 0.07. Values reported in the literature are 0,761+-5.52% by Brand et al., 2020 and 0.594 by Vaysi and Tajik, 2015. Altought precise values for *P.Aureosulcata* were not found in the literature, in general, bamboo density is contained between 0.4 and 0.9 $gr*cm^{-3}$ (Chaowana, 2013). Even if this represent a wide range of values, it assures that the results obtained here are not out of range.

Gutu, 2013, indicates that the density in bamboo changes with its age. It increases from 1 to 6 years, then stay more stable until 8, after that, it encounters a small decrease. In 7 other bamboo species (*Bambusa vulgaris var. vulgaris, Bambusa vulgaris var. striata, Bambusa balcooa, Bambusa tulda, Bambusa polymorpha, Dendrocalamus strictus, Bambusa bambos* and *Phyllostachys pubescens*), Selvan et al., 2017 and Berndsen et al., 2010, also observed an increase in basic density with age. Some studies also pointed out the variations in specific gravity due to climatic factors, edaphic factors, and localization, suggesting the importance of the use of habitat specific values for specific gravity (Pati et al., 2022; Wiemann & Williamson, 2002). In addition, it is also indicated that the density of nodes is higher than the density of internodes (Chaowana, 2013).

Due to those factors, it is complicated to precisely compare the basic density of the results from this study with other references. However, knowing that the culms observed in this work are considered young it can be questionable to obtain higher values than the afore-cited studies. Moreover, nodes and internodes densities (Figure 16) returned results contradictory to what is said in literature. Explanations for those differences can potentially be found in manipulations approximations. To begin with, it is possible that culms samples were not optimally fresh during the volume measurements. The measurements were done as soon as possible, and the samples were correctly sealed. However, some time has passed between the sampling of the bamboos and the volume measurements. In addition, this happened during period with warm temperatures. It is then possible that the culms began to dry during this period. The drying itself could have generated a volume shrinkage. A volume diminution would diminish the fresh volume term in the basic density equation. This could cause an overestimation of the basic density value. In response to this potential issue, a small Moisture Content measurement was done (See Appendix E for data). This test returned values between 27.78 and 77.87% for internodes, 19.87 and 53.92 % for nodes and a total mean between 23.82 and 61.84%. Shrinkage begins to occurs below the fiber saturation point. Generally it is estimated to be around 30% (Reeb, 1995). Most of the samples seems to be above 30%, so this could refute the shrinkage hypothesis. Regarding the difference in basic density between nodes and internodes, it is imaginable that nodes volumes were overestimated because of the presence of air bubbles which increase the volume (thus decrease the basic density). Because of their shape, the difficulty was indeed higher to expel air bubbles from the nodes compared to the internodes and the volumes measured were sometimes really small. This could potentially cause overestimation of nodes volumes, so an underestimation of their basic density.

2 Modelling and performance parameters of validated models

For all species nonlinear regression returned the most validated models, only 3/12 validated models were linear regression models. Although linear models for AGB can be fit using log, in the case of this study it seems the linear regression is way less effective than nonlinear regression. The species returning the most validated model was *P.Nigra* (4) and the species returning the least number of validated models was *P.Aureosulcata*(2). An explanation could be the number of samples used for the modelling of the relationship between AGB and the inputs variables. Huy and Long, 2019, recommend the sampling of minimum 30 culms for the creation of an allometric equation. Although it succeeded with 10 samples for *P.Aurea* and *P.Nigra*, it seems to be an already small number for this procedure. The reduction of samples for *P.Aureosulcata* (N data = 9) due to an invalid measurement exacerbated the modeling difficulties especially during the cross-validation. Regarding the multi species model, it only produced 3 validated models, but this is due to preselection. Multispecies models had the highest number of qualified models overall, but formulas of the same type were preselected before cross-validation. This means that between identical formulas for one type of model, only one was selected for cross validation. This was based on parameters quality (high R2adjusted and low AIC).

Globally, adding variables during the modelling produced a better fit (Tables 17,18, 19, 20) but fewer qualified model. This is due to regression computation difficulties in the program R. Once again, a small samples number (10 or 9) is not optimal for the use of regression. Furthermore, the high collinearity between the DBH and the height in the data, added complication to the regression's computation. In the end, the most used variable in validated models is the H variable, followed by DBH. Basic density comes last, but it was only tested as a secondary variable. In general, DBH is the most used variable for predicting AGB in bamboos (Appendix A).

In APPENDIX A it can be found that R^2 found in this large range of studies oscillates between 0.998 to 0.488. In comparison, validated models in the present study returned mostly values higher than 0.9. The only two lower values of R^2 come from *P.Nigra M1* and *M2* (Table 3) and are respectively 0.798 (the lowest value) and 0.811. The highest value is 0.982 and comes from *P.Aurea, A1.* Those high r-squared values indicates that the models fit the data well. A better model fit indication can be found in R^2_{adj}. Abebe et al., 2023, resume his and others study (Amoah et al., 2020; Mulatu & Fetene, 2013) about AGB modelling for bamboo in the following table (Table 9):

Table 9: Model validation of 4 different species from 3 studies (derived from Abebe et al., 2023).

Source	Species specific	Model	adj.R^2
Abebe et al. (2023)	*Oldeania alpina*	AGB $=0.259\times(\text{D})^{2.098}$	0.925
		AGB $=0.139\times(\text{D})^{2.577}$	0.856
		AGB $=0.165\times(\text{D})^{2.487}$	0.922
Mulatu and Fetene (2013)	*Oldeania alpina*	AGB=exp $(0.172\times\text{D})$	0.87
		AGB=exp $(0.289\times\text{D})$	0.87
		AGB=exp $(0.30\times\text{D})$	0.99
Amoah et al. (2020)	*Bambusa vulgaris*	AGB$=0.763\times(\text{D})^{1.84}$	0.971
		AGB$=0.291\times(\text{D})^{2.26}$	0.926
		AGB$=0.061\times(\text{D})^{2.883}$	0.955
Amoah et al. (2020)	*Oxytenanthera abyssinica*	AGB$=2.632\times(\text{D})^{1.881}$	0.955
		AGB$=1.910\times(\text{D})^{2.410}$	0.855
		AGB$=2.304\times(\text{D})^{2.233}$	0.919

For those equations, R^2_{adj} values varies from 0.855 to 0.990. In the case of the present study, the minimum R^2_{adj} measured was 0.697 and the maximum was 0.976. Once again, this shows a relatively good fit of the model even when taking account of the numbers of input variables. In their guidelines, UNFCCC, 2011, advised a minimum determination coefficient value of 0.85. This assumption is verified for all models except for the two first models of *P.Nigra (N1, N2).*

The biases (%) reported here were almost all negative (except *P.Aurea A3*) and with a maximum absolute value of 7.211. The highest and lowest biases absolute valor measurement occurred repectively for *P.Nigra N1* and for *P.Aurea A3.* In this case, a negative bias mean that the models tend to overestimate the AGB.

The RMSE (*kg*) ranged between 0.050 (*P.Aurea A1, A2*) to 0.158 (Multi-species *M1*). It represents a 3-fold difference. However, it is important to remember that the range of the sample used for the 4 types of equation were different. The mixed species model had AGB (*kg*) data points ranging from 0.06 to 2.67. While the *P.Aurea*, *P.Aureosulcata* and *P.Nigra* ranged respectively between 0.07 and 1.19 kg, 0.2 and 2.67 *kg*, and 0.06 and 1 *kg*.

Lastly the MAPE (%) returned values from 6.991 to 24.913 for all selected models. The highest MAPE was attributed to model *P.Nigra N1* and the lowest MAPE value was attributed to *P.Aurea A3*. By looking at the MAPE values, it seems that increasing the numbers of variables inputs tended to decrease the MAPE. Other studies reported MAPE values for the modeling of bamboo AGB; Li et al., 2016, tested 4 models producing MAPE from 11.54% to 18.22%; Huy et al., 2019, tested 8 different combinations models returning values between 27.1 and 30.5%; Yebeyen et al., 2022, tested 10 models and returned values of MAPE between 4.0 and 8.1. The values we obtained in this study seems to be comparable with them.

In the end a good allometry model should not only display good parameters (R^2, RMSE,...) but should tend to be the simplest, the more generalized, and the most robust possible. Multiple model choices are available here. Regarding generalization, the multi-species model should be considered. However, it is important to keep in mind that all DBH distributions are considered non-equal and that H distributions of *P.Nigra* is also different from the two others distributions. Regarding simplicity, the models with only one input parameter should be considered. Furthermore, in practice, the variables that are easier to measure are in order, DBH, H and basic density. Density is also an input that is obtained destructively. However, it could still be used as a constant from a small sampling or from databases. About robustness, all the selected models have been put through cross-validation. Although the number of samples and the number of iterations could have been higher; it still describes a good robustness of the models. If one would use those allometric equations. It is still important to consider the range of data from which the equations were build.

3 Aboveground Biomass and Carbon Stock and Sink estimation via selected models.

The AGB and C stock measured thanks to the volume approximation (Table 5) returned values between 6.53 to 34.17 $tonC{\cdot}ha^{-1}$ which seems higher than the estimation with models. However, if we only take into account the basic values (culm, not multiplied by 1.3) it falls closer to the ranges observed with the models estimation. This could be a good indication of coherent estimations.

Globally, the carbon stock estimation by models oscillated between 4.455 +- 0.562 $ton{\cdot}ha^{-1}$ for *N3* to 24.611 +- 2.005 $ton{\cdot}ha^{-1}$ for *A3* (Table6). The multi species model produced estimations between 14.639 +- 0.616 and 19.328 +- 0.337 $ton{\cdot}ha^{-1}$; the *P.Aurea* models from 18.957 +- 1.264 to 24.611 +- 2.005; the *P.Nigra* models from 4.455 +- 0.562 to 15.171 +- 0.514; and the two *P.Aureosulcata* models showed estimates of 11.965 +- 0.627 and 13.166 +- 0.656. *P.Aurea* produced the greatest C stock estimates of the 3 species. It does not possess the biggest culms of the 3 species so this is mainly due to its culm density. Here, the culm density of *P.Aurea* is by far greater than the two other. The impact of culm density on AGB estimations was also observed in Chen et al., 2009; Nath and Das, 2011. In fact, lower culm densities usually result in higher DBH but cause a decrease in biomass per area, while higher culm densities are related to lower DBH but higher biomass (Kleinhenz & Midmore, 2001). This explain why despite being way bigger than *P.Aurea*, *P.Aureosulcata* seems to have less AGB per unit area. Once again due to the young stage of the *P.Nigra* stand, it seems to represent less AGB per unit area than his two competitors. However, it is important to note the high variability between the different AGB estimations of *P.Nigra*. As it have been explain previously, *P.Nigra* models were the ones with the lowest quality overall this could probably partially explain those variations.

Yuen et al., 2017, did an extensive study about C stocks in bamboo ecosystems worldwide. It shows that Carbon stock between species, depending on the annual rainfall, mean temperature, and culm density can vary greatly. To help comparison, a small resume table (Table 10) can be found here:

Table 10: Annual rainfall (mm) an mean annual temperature (°C) at Merksplas, BELGIUM. In parrallel with Mean AGCarbon estimation in $ton{\cdot}ha^{-1}$ and culm density in culm$\cdot ha^{-1}$

SPECIES	Mean AGC estimation (Ton*ha^{-1})	Annual rainfall (mm)	Mean annual temperature (°C)	Culm density . (culms*ha^{-1})
Multi-Species	16.21	893.5	10.8	61272
P.Aurea	22.17	893.5	10.8	141032
P.Aureosulcata	12.57	893.5	10.8	40944
P.Nigra	8.71	893.5	10.8	55878

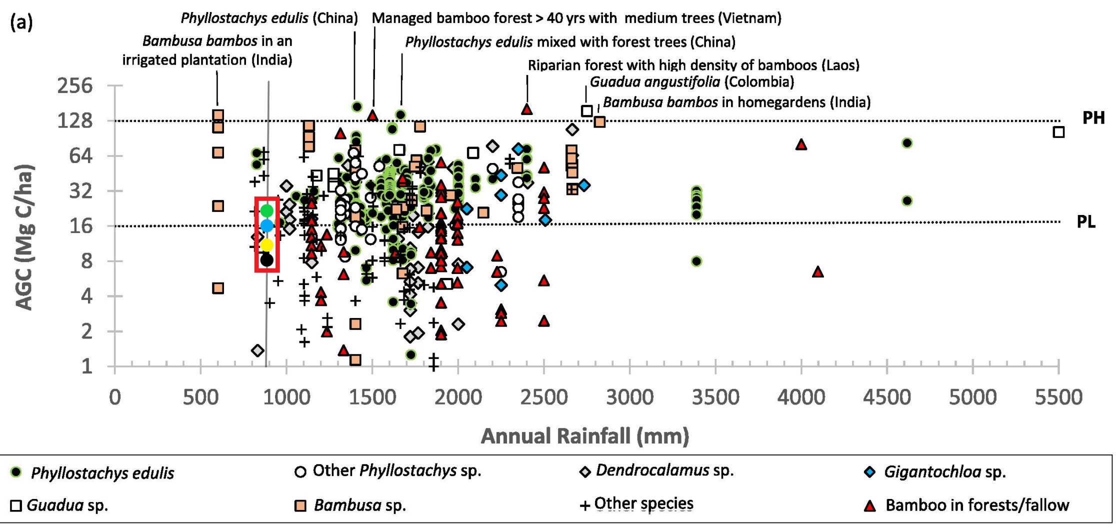

Figure 24: Derived figures from Yuen et al., 2017, with approximate positioning of *P.Aurea* (in green), *P.Aureosulcata* (in yellow), *P.Nigra* (in black) and mixed species model (in blue) Above ground carbon estimations $ton{\cdot}ha^{-1}$ reported with annual rainfall (mm).

Having less precipitation and a smaller mean annual temperature than most of the plotted values, the estimations made in this study come around the plausible low (PL) point. This point represent the low range threshold that the study consider for a range of environmental and management conditions supposedly associated with healthy stands of

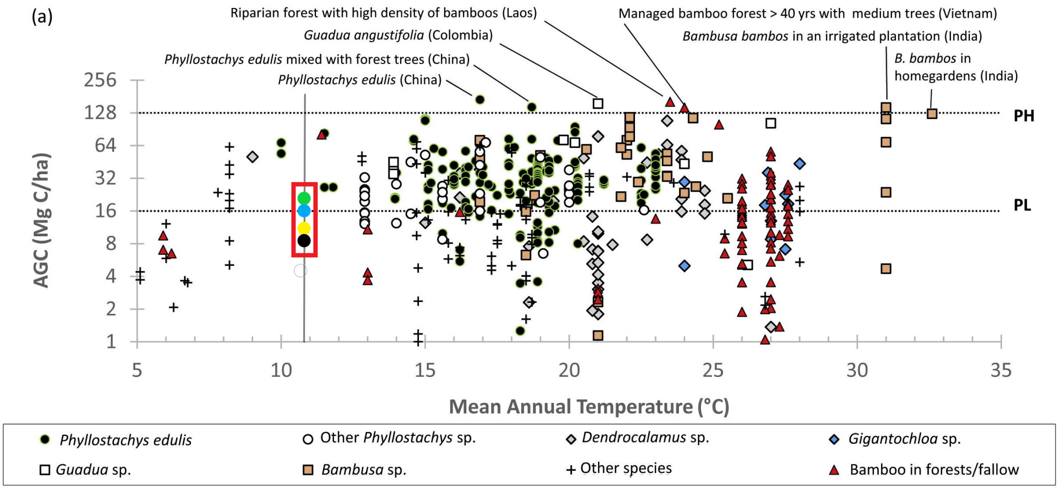

Figure 25: Derived figures from Yuen et al., 2017, with approximate positioning of *P.Aurea* (in green), *P.Aureosulcata* (in yellow), *P.Nigra* (in black) and mixed species model (in blue) Above ground carbon estimations $ton{\cdot}ha^{-1}$ reported with Mean annual temperature (°C).

different types of bamboo. The majority of the other *Phyllostachys* species seems to have a higher estimation of AGC stock. Although the 3 estimated AGC stocks seems bellow most other studies they still are of interest especially due to the difference in climate with other species. It is also important to note that all the other studies are from Asia or South America. It was also difficult to compare the AGC in relation with culm density. The authors limited the range of the culm densities explaining that culms by squared meter transposed to culms by *ha* produced values too large.

The study of new shoots Carbon sink (Table 8) returned values ranging from 0.509 +- 0.116 (*P.Aurea a1*) to 2.925 +- 0.215 (*P.Nigra p2*). Those value can be considered as an estimation of this year new carbon sink. However, growth was probably not finished when measuring new shoots. First of all, it was visible that some culms just happened to emerge. In addition, a comparison between adult (Table 2) and young (Table 7) new culms DBH and H data show a difference between them. This indicate that the estimation is possibly underestimating the true carbon sink. The Carbon stock values obtained here seems to be opposed to the values obtained before regarding AGB estimates. Here *P.Aurea* shows the lowest value and *P.Nigra* the highest. This is mainly due to the number of culms measured. The new shoots culm density was indeed higher for *P.Nigra*. This observation may seems counter intuitive but is probably due to the resources availability in the *P.Nigra* bamboo stands. Having a young bamboo stand with fewer adult culms probably reduce the resources competition for young culms.

V Conclusion & *Prospects*

1 Conlusion

The ambition of this study was to assess bamboo AGB and C stock for three different species: *Phyllostachys Aurea*, *Phyllostachys Aureosulcata* and *Phyllostachys Nigra*.

Allometric equations were proposed after the study of the input parameters, Diameter at Breast Height, Height, Basic density, and the test of multiple models. The allometric equations selected in this work showed very good performance metrics except for two models, *P.Nigra N1* and *N2* that returned slightly poorer results.

The assessment of Aboveground Biomass with the selected models returned estimated values ranging from 9.48 ± 1.19 to 52.36 ± 4.26 $tonAGB{\cdot}ha^{-1}$ depending on model and species. This translate to 4.45 ± 0.56 to 24.61± 2.00 $tonC{\cdot}ha^{-1}$ The species with the higher values was *P.Aurea* and the one with the lowest values was *P.Nigra*. One key componant of the high *P.Aurea* AGB estimation seems to be his high Culm Density compared to his peers.

The estimation of the potential yearly sink of C gave results ranging between 0.51 ± 0.12 and 2.96 ± 0.21 $tonC{\cdot}ha^{-1}$. This time the species with the most potential was *P.Nigra* and the one with the lowest yearly C sink was *P.Aurea*. The yearly C sinks values were probably underestimated due to an unfinished growing season at the time of measurements.

When using those equations, one should keep in mind the limitations of those models. The modelling was based on a small number of samples (between 29 and 9 depending on the model) describing the entirety of the DBH distribution. It is also possible that basic density measurements were overestimated. In addition, the potential user of those equations should pay attention to the DBH and H ranges on which those equations were build. However, the species observed in this work don't seem to have been studied regarding biomass production. Additionally, bamboo AGB allometric equation adapted and studied in the climate zone of Europe seems to be almost nonexistent. So, the equations proposed here could be of great utility.

2 Prospects

While this study has made significant strides in assessing bamboo's Above-Ground Biomass (AGB) and carbon stock across three distinct species in the Belgian context, several promising research paths emerge for the future.
To begin with, it would be interesting to further explore allometric equations by possibly incorporating additional input parameters and addressing the eventual lack of data. An important point would also be to further study the basic density in those species. It would

allow a better understanding of the model and the impact of this variable. In short, it could enhance the accuracy and applicability of AGB and carbon stock estimation models.

Optionnaly, engaging in long-term validation efforts could contribute to the establishment of a robust foundation for carbon stock estimation. This continuous assessment of model accuracy, when compared with real-world measurements over time, could ensure the equations remain.

Another interesting point could be a deeper exploration of optimal bamboo management practices. As it seems that management is a key aspect in the C sequestration potential.Investigating of factors like planting density, culm density, and habitat conditions could guide sustainable bamboo cultivation practices that align with carbon storage goals.

In summary, the developed allometric equations, while generally robust, invite future refinement. Through these experimentation's, more can be learned about bamboo's role in global climate change mitigation.

References

Abebe, S., Gebeyehu, G., Teketay, D., Long, T. T., & Jayaraman, D. (2023). Allometric models for estimating biomass storage and carbon stock potential of oldeania alpina (k. schum.) stapleton forests of south-western ethiopia. *Advances in Bamboo Science*, *2*, 100008. https://doi.org/10.1016/j.bamboo.2022.100008

Ahmad, Z., Upadhyay, A., Ding, Y., Emamverdian, A., & Shahzad, A. (2021). Bamboo: Origin, habitat, distributions and global prospective. In Z. Ahmad, Y. Ding, & A. Shahzad (Eds.), *Biotechnological advances in bamboo: The "green gold" on the earth* (pp. 1–31). Springer. https://doi.org/10.1007/978-981-16-1310-4_1

Akaike, H. (n.d.). Information theory and an extension of IthnefoMrmaaxtiimonumTh-LeiokreyliahnododanPrEinxcteipnlseion of the maximum likelihood principle.

Akinlabi, E. T., Anane-Fenin, K., & Akwada, D. R. (2017). *Bamboo*. Springer International Publishing. https://doi.org/10.1007/978-3-319-56808-9

Al-Mamoori, A., Krishnamurthy, A., Rownaghi, A. A., & Rezaei, F. (2017). Carbon capture and utilization update. *Energy Technology*, *5*(6), 834–849. https://doi.org/10.1002/ente.201600747

Amoah, M., Assan, F., & Dadzie, P. K. (2020). Aboveground biomass, carbon storage and fuel values of bambusa vulgaris, oxynanteria abbyssinica and bambusa vulgaris var.vitata plantations in the bobiri forest reserve of ghana. *Journal of Sustainable Forestry*, *39*(2), 113–136. https://doi.org/10.1080/10549811.2019.1608452

Basuki, T. M., van Laake, P. E., Skidmore, A. K., & Hussin, Y. A. (2009). Allometric equations for estimating the above-ground biomass in tropical lowland dipterocarp forests. *Forest Ecology and Management*, *257*(8), 1684–1694. https://doi.org/10.1016/j.foreco.2009.01.027

Ben-zhi, Z., Mao-yi, F., Jin-zhong, X., Xiao-sheng, Y., & Zheng-cai, L. (2005). Ecological functions of bamboo forest: Research and application. *Journal of Forestry Research*, *16*(2), 143–147. https://doi.org/10.1007/BF02857909

Berndsen, R. S., Klitzke, R. J., Batista, D. C., Nascimento, E. M. D., & Ostapiv, F. (2010). PROPRIEDADES FÍSICAS DO BAMBU-MOSSÔ (phyllostachys pubescens mazel ex h. de lehaie) EM DIFERENTES IDADES e POSIÇÕES DO COLMO. *RF*, *40*(1). https://doi.org/10.5380/rf.v40i1.17109

Brand, M. A., Gaa, A. Z. N., Balduino Junior, A. L., Cunha, A. B. D., & Rios, P. D. (2020). Potencial do uso de quatro espécies de bambu para a produção de carvão vegetal para uso doméstico. *Ciênc. Florest.*, *30*(1), 60. https://doi.org/10.5902/1980509827348

Cao, L., Coops, N. C., Sun, Y., Ruan, H., Wang, G., Dai, J., & She, G. (2019). Estimating canopy structure and biomass in bamboo forests using airborne LiDAR data. *ISPRS Journal of Photogrammetry and Remote Sensing*, *148*, 114–129. https://doi.org/10.1016/j.isprsjprs.2018.12.006

Cavanaugh, J. E., & Neath, A. A. (2019). The akaike information criterion: Background, derivation, properties, application, interpretation, and refinements. *WIREs Comp Stat*, *11*(3). https://doi.org/10.1002/wics.1460

Chaowana, P. (2013). Bamboo: An alternative raw material for wood and wood-based composites. *JMSR*, *2*(2), p90. https://doi.org/10.5539/jmsr.v2n2p90

Chave, J., Andalo, C., Brown, S., Cairns, M. A., Chambers, J. Q., Eamus, D., Fölster, H., Fromard, F., Higuchi, N., Kira, T., Lescure, J.-P., Nelson, B. W., Ogawa, H., Puig, H., Riéra, B., & Yamakura, T. (2005). Tree allometry and improved estimation of carbon stocks and balance in tropical forests. *Oecologia*, *145*(1), 87–99. https://doi.org/10.1007/s00442-005-0100-x

Chave, J., Réjou-Méchain, M., Búrquez, A., Chidumayo, E., Colgan, M. S., Delitti, W. B., Duque, A., Eid, T., Fearnside, P. M., Goodman, R. C., Henry, M., Martínez-Yrízar, A., Mugasha, W. A., Muller-Landau, H. C., Mencuccini, M., Nelson, B. W., Ngomanda, A., Nogueira, E. M., Ortiz-Malavassi, E., . . . Vieilledent, G. (2014). Improved allometric models to estimate the aboveground biomass of tropical trees. *Global Change Biology*, *20*(10), 3177–3190. https://doi.org/10.1111/gcb.12629

Chen, X., Zhang, X., Zhang, Y., Booth, T., & He, X. (2009). Changes of carbon stocks in bamboo stands in china during 100 years. *Forest Ecology and Management*, *258*(7), 1489–1496. https://doi.org/10.1016/j.foreco.2009.06.051

Devi, A. S., & Singh, K. S. (2021). Carbon storage and sequestration potential in aboveground biomass of bamboos in north east india. *Sci Rep*, *11*(1), 837. https://doi.org/10.1038/s41598-020-80887-w

Dlugokencky, E., & Tans, P. (2023). *Trends in atmospheric carbon dioxide*. National Oceanic and Atmospheric Administration, Global Monitoring Laboratory (NOAA/GML). https://gml.noaa.gov/ccgg/trends/global.html

FAO. (2020a). *Global forest resources assessment 2020: Main report*. https://doi.org/10.4060/ca9825en

FAO. (2020b). Global forest resources assessment, terms and definitions.

Fawzy, S., Osman, A. I., Doran, J., & Rooney, D. W. (2020). Strategies for mitigation of climate change: A review. *Environ Chem Lett*, *18*(6), 2069–2094. https://doi.org/10.1007/s10311-020-01059-w

Flora of china: Bambusoideae. (n.d.). http://www.efloras.org/florataxon.aspx?flora_id=2&taxon_id=242337528

Friedlingstein, P., O'Sullivan, M., Jones, M. W., Andrew, R. M., Gregor, L., Hauck, J., Le Quéré, C., Luijkx, I. T., Olsen, A., Peters, G. P., Peters, W., Pongratz, J., Schwingshackl, C., Sitch, S., Canadell, J. G., Ciais, P., Jackson, R. B., Alin, S. R., Alkama, R., . . . Zheng, B. (2022). Global carbon budget 2022. *Earth System Science Data*, *14*(11), 4811–4900. https://doi.org/10.5194/essd-14-4811-2022

Gangwar, T., & Schillinger, D. (2019). Microimaging-informed continuum micromechanics accurately predicts macroscopic stiffness and strength properties of hierarchical plant culm materials. *Mechanics of Materials*, *130*, 39–57. https://doi.org/10.1016/j.mechmat.2019.01.009

Gielis, J. (2023). Future possibilities for bamboo in european agriculture.

Gutu, T. (2013). A study on the mechanical strength properties of bamboo to enhance its diversification on its utilization. *2*(5).

Heimann, M., & Reichstein, M. (2008). Terrestrial ecosystem carbon dynamics and climate feedbacks. *451*.

Hou, G., Delang, C. O., Lu, X., & Olschewski, R. (2019). Valuing carbon sequestration to finance afforestation projects in china. *Forests*, *10*(9), 754. https://doi.org/10.3390/f10090754

Houghton, R. (2007). Balancing the global carbon budget. *Annu. Rev. Earth Planet. Sci.*, *35*(1), 313–347. https://doi.org/10.1146/annurev.earth.35.031306.140057

Hughes, S. W. (2005). Archimedes revisited: A faster, better, cheaper method of accurately measuring the volume of small objects. *Phys. Educ.*, *40*(5), 468–474. https://doi.org/10.1088/0031-9120/40/5/008

Huy, B., Kralicek, K., Poudel, K. P., Phuong, V. T., Khoa, P. V., Hung, N. D., & Temesgen, H. (2016a). Allometric equations for estimating tree aboveground biomass in evergreen broadleaf forests of viet nam. *Forest Ecology and Management*, *382*, 193–205. https://doi.org/10.1016/j.foreco.2016.10.021

Huy, B., & Long, T. (2019, June 12). *A manual for bamboo forest biomass and carbon assessment*.

Huy, B., Poudel, K. P., Kralicek, K., Hung, N. D., Khoa, P. V., Phng, V. T., & Temesgen, H. (2016b). Allometric equations for estimating tree aboveground biomass in tropical dipterocarp forests of vietnam. *Forests*, *7*(8), 180. https://doi.org/10.3390/f7080180

Huy, B., Thanh, G. T., Poudel, K. P., & Temesgen, H. (2019). Individual plant allometric equations for estimating aboveground biomass and its components for a common bamboo species (bambusa procera a. chev. and a. camus) in tropical forests. *Forests*, *10*(4), 316. https://doi.org/10.3390/f10040316

IPCC. (2021). Summary for policymakers. In V. Masson-Delmotte, P. Zhai, A. Pirani, S. L. Connors, C. Péan, S. Berger, N. Caud, Y. Chen, L. Goldfarb, M. I. Gomis, M. Huang, K. Leitzell, E. Lonnoy, J. B. R. Matthews, T. K. Maycock, T. Waterfield, O. Yelekçi, R. Yu, & B. Zhou (Eds.), *Climate change 2021: The physical science basis. contribution of working group i to the sixth assessment report of the intergovernmental panel on climate change*. Cambridge University Press. https://doi.org/10.1017/9781009157896.001

Keenan, T., & Williams, C. (2018). The terrestrial carbon sink. *Annu. Rev. Environ. Resour.*, *43*(1), 219–243. https://doi.org/10.1146/annurev-environ-102017-030204

Kleinhenz, V., & Midmore, D. J. (2001). Aspects of bamboo agronomy. In *Advances in agronomy* (pp. 99–153). Elsevier. https://doi.org/10.1016/S0065-2113(01)74032-1

Kovacs, N. (2022). Study of soil carbon dynamics under a bamboo plantation in Belgium.

Kuehl, Y., Li, Y., & Henley, G. (2013). Impacts of selective harvest on the carbon sequestration potential in moso bamboo (phyllostachys pubescens) plantations. https://doi.org/https://doi.org/10.1080/14728028.2013.773652

Lawrence, M. G., Schäfer, S., Muri, H., Scott, V., Oschlies, A., Vaughan, N. E., Boucher, O., Schmidt, H., Haywood, J., & Scheffran, J. (2018). Evaluating climate geoengineering proposals in the context of the paris agreement temperature goals. *Nat Commun*, *9*(1), 3734. https://doi.org/10.1038/s41467-018-05938-3

Le Quéré, C., Peters, G. P., Friedlingstein, P., Andrew, R. M., Canadell, J. G., Davis, S. J., Jackson, R. B., & Jones, M. W. (2021). Fossil CO2 emissions in the post-COVID-19 era. *Nat. Clim. Chang.*, *11*(3), 197–199. https://doi.org/10.1038/s41558-021-01001-0

Li, L.-E., Lin, Y.-J., & Yen, T.-M. (2016). Using allometric models to predict the aboveground biomass of thorny bamboo (bambusa stenostachya) and estimate its carbon storage.

Li, P., Zhou, G., Du, H., Lu, D., Mo, L., Xu, X., Shi, Y., & Zhou, Y. (2015). Current and potential carbon stocks in moso bamboo forests in china. *Journal of Environmental Management*, *156*, 89–96. https://doi.org/10.1016/j.jenvman.2015.03.030

Liese, W., & Köhl, M. (Eds.). (2015). *Bamboo: The plant and its uses* (Vol. 10). Springer International Publishing. https://doi.org/10.1007/978-3-319-14133-6

Lieurance, D., Cooper, A., Young, A. L., Gordon, D. R., & Flory, S. L. (2018). Running bamboo species pose a greater invasion risk than clumping bamboo species in the continental united states. *Journal for Nature Conservation*, *43*, 39–45. https://doi.org/10.1016/j.jnc.2018.02.012

Mayer, D. G., & Butler, D. G. (1993). Statistical validation. *Ecological Modelling*, *68*(1), 21–32. https://doi.org/10.1016/0304-3800(93)90105-2

Mbamu, M. F. A. D. O., Nascimento, A. M. D., Garcia, R. A., Jesus, D. S. D., & Souza Junior, A. D. D. (2020). Propriedades físicas dos bambus das espécies Phyllostachys aurea e Bambusa tuldoides após tratamento térmico. *RCM*, *11*(2), 85–92. https://doi.org/10.12953/2177-6830/rcm.v11n2p85-92

Mera, F. A. T., & Xu, C. (2014). PLANTATION MANAGEMENT AND BAMBOO RESOURCE ECONOMICS IN CHINA. *Ciencia y Tecnología.*

Mulatu, Y., & Fetene, M. (2013). STAND STRUCTURE, GROWTH AND BIOMASS OF ARUNDINARIA ALPINA (HIGHLAND BAMBOO) ALONG TOPOGRAPHIC GRADIENT IN THE CHOKE MOUNTAIN, NORTHWESTERN ETHIOPIA. *Ethiopian Journal of Biological Sciences*, *12*(1), 1–23.

Nath, A. J., & Das, A. K. (2011). Carbon storage and sequestration in bamboo-based smallholder homegardens of barak valley, assam. *Current Science*, *100*(2), 229–233.

Nath, A. J., Lal, R., & Das, A. K. (2015). Managing woody bamboos for carbon farming and carbon trading. *Global Ecology and Conservation*, *3*, 654–663. https://doi.org/10.1016/j.gecco.2015.03.002

Norby, R. J., DeLucia, E. H., Gielen, B., Calfapietra, C., Giardina, C. P., King, J. S., Ledford, J., McCarthy, H. R., Moore, D. J. P., Ceulemans, R., De Angelis, P., Finzi, A. C., Karnosky, D. F., Kubiske, M. E., Lukac, M., Pregitzer, K. S., Scarascia-Mugnozza, G. E., Schlesinger, W. H., & Oren, R. (2005). Forest response to elevated CO $_2$ is conserved across a broad range of productivity. *Proc. Natl. Acad. Sci. U.S.A.*, *102*(50), 18052–18056. https://doi.org/10.1073/pnas.0509478102

Pan, Y., Birdsey, R. A., Fang, J., Houghton, R., Kauppi, P. E., Kurz, W. A., Phillips, O. L., Shvidenko, A., Lewis, S. L., Canadell, J. G., Ciais, P., Jackson, R. B., Pacala, S. W., McGuire, A. D., Piao, S., Rautiainen, A., Sitch, S., & Hayes, D. (2011). A large and persistent carbon sink in the world's forests. *Science*, *333*(6045), 988–993. https://doi.org/10.1126/science.1201609

Pati, P., Kaushik, P., Khan, M., & Khare, P. (2022). Wood specific gravity in indian forests: A review. *International Journal of Ecology and Environmental Sciences*, *48*, 143–164. https://doi.org/10.55863/ijees.2022.0111

Picard, N., Rutishauser, E., Ploton, P., Ngomanda, A., & Henry, M. (2015). Should tree biomass allometry be restricted to power models? *Forest Ecology and Management*, *353*, 156–163. https://doi.org/10.1016/j.foreco.2015.05.035

Poudel, K., & Temesgen, H. (2016). Methods for estimating aboveground biomass and its components for douglas-fir and lodgepole pine trees. *Can. J. For. Res.*, *46*(1), 77–87. https://doi.org/10.1139/cjfr-2015-0256

Reeb, J. E. (1995). Wood and moisture relationships.

Ricke, K. L., Millar, R. J., & MacMartin, D. G. (2017). Constraints on global temperature target overshoot. *Sci Rep*, *7*(1), 14743. https://doi.org/10.1038/s41598-017-14503-9

RMI, Royal Meteorological Institute of Belgium. (n.d.). *Climat dans votre commune*. RMI. https://www.meteo.be/fr/climat/climat-de-la-belgique/climat-dans-votre-commune

Rusch, F., De Abreu Neto, R., De Moraes Lúcio, D., & Hillig, É. (2021). Energy properties of bamboo biomass and mate co-products. *SN Appl. Sci.*, *3*(6), 602. https://doi.org/10.1007/s42452-021-04584-7

Scharlemann, J. P., Tanner, E. V., Hiederer, R., & Kapos, V. (2014). Global soil carbon: Understanding and managing the largest terrestrial carbon pool. *Carbon Management*, *5*(1), 81–91. https://doi.org/10.4155/cmt.13.77

Selvan, R. T., Parthiban, K. T., & Khanna, S. U. (2017). Physio-chemical properties of bamboo genetic resources at various age gradations. *Int.J.Curr.Microbiol.App.Sci.*, *6*(9), 1671–1681. https://doi.org/10.20546/ijcmas.2017.609.205

Sette Júnior, C. R., Lima, P. A. F., Lopes, D. M. M., Barbosa, P. V. G., Coneglian, A., & Almeida, R. D. A. (2017). Characterization of biomass, charcoal and briquette of phyllostachys aurea carr. ex a. & c. rivière. *Sci. For.*, *45*(116). https://doi.org/10.18671/scifor.v45n116.03

Song, X., Zhou, G., Jiang, H., Yu, S., Fu, J., Li, W., Wang, W., Ma, Z., & Peng, C. (2011). Carbon sequestration by chinese bamboo forests and their ecological benefits: Assessment of potential, problems, and future challenges. *Environ. Rev.*, *19*, 418–428. https://doi.org/10.1139/a11-015

Soreng, R. J., Peterson, P. M., Zuloaga, F. O., Romaschenko, K., Clark, L. G., Teisher, J. K., Gillespie, L. J., Barberá, P., Welker, C. A. D., Kellogg, E. A., Li, D.-Z., & Davidse, G. (2022). A worldwide phylogenetic classification of the poaceae (gramineae) III: An update. *J of Sytematics Evolution*, *60*(3), 476–521. https://doi.org/10.1111/jse.12847

Troya Mera, F. A., & Xu, C. (2014). PLANTATION MANAGEMENT AND BAMBOO RESOURCE ECONOMICS IN CHINA. *CyT*, *7*(1), 1–12. https://doi.org/10.18779/cyt.v7i1.93

UNFCCC. (n.d.). *Unfccc greenhouse gas data - global warming potentials*. Retrieved August 14, 2023, from https://unfccc.int/process/transparency-and-reporting/greenhouse-gas-data/greenhouse-gas-data-unfccc/global-warming-potentials

UNFCCC. (2011). *A/r methodological tool: Demonstrating appropriateness of allometric equations for estimation of aboveground tree biomass in a/r cdm project activities (version 01.0.0)*. https://cdm.unfccc.int/methodologies/ARmethodologies/tools/ar-am-tool-17-v1.pdf

UNFCCC. (2023). Cop27 cover decision, https://unfccc.int/sites/default/files/resource/cop27-cover-decision.pdf.

Van Der Gaast, W., Sikkema, R., & Vohrer, M. (2018). The contribution of forest carbon credit projects to addressing the climate change challenge. *Climate Policy*, *18*(1), 42–48. https://doi.org/10.1080/14693062.2016.1242056

Vaysi, R., & Tajik, M. (2015). An investigation on the physical, chemical, and biometrical properties of planted bamboo.

Vorontsova, M., Clark, L., Dransfield, J., Govaerts, R., & Baker, W. (2016a, December 31). *World checklist of bamboos and rattans*.

Vorontsova, M., Clark, L., Dransfield, J., Govaerts, R., Wilkinson, T., & Baker, W. (2016b, December 31). *World atlas of bamboos and rattans*.

Wiemann, M. C., & Williamson, G. B. (2002). Geographic variation in wood specific gravity: Effects of latitude, temperature, and precipitation. *Wood and Fiber Science*, 96–107.

Xu, M., Ji, H., & Zhuang, S. (2018). Carbon stock of moso bamboo (phyllostachys pubescens) forests along a latitude gradient in the subtropical region of china (A. Nath, Ed.). *PLoS ONE*, *13*(2), e0193024. https://doi.org/10.1371/journal.pone.0193024

Xu, X., Xu, P., Zhu, J., Li, H., & Xiong, Z. (2022). Bamboo construction materials: Carbon storage and potential to reduce associated CO2 emissions. *Science of The Total Environment*, *814*, 152697. https://doi.org/10.1016/j.scitotenv.2021.152697

Yebeyen, D., Nemomissa, S., Sileshi, G. W., Zewdie, W., Hailu, B. T., Rodríguez, R. L., Desalegne, F. H., & Woldie, T. M. (2022). Allometric scaling, biomass accumulation and carbon stocks in natural highland bamboo (oldeania alpina (k. schum.) stapleton) stands in southwestern ethiopia. *Carbon Management*, *13*(1), 482–496. https://doi.org/10.1080/17583004.2022.2130090

Yen, T.-M. (2016). Culm height development, biomass accumulation and carbon storage in an initial growth stage for a fast-growing moso bamboo (phyllostachy pubescens). *Bot Stud*, *57*(1), 10. https://doi.org/10.1186/s40529-016-0126-x

Yen, T.-M., Ji, Y.-J., & Lee, J.-S. (2010). Estimating biomass production and carbon storage for a fast-growing makino bamboo (phyllostachys makinoi) plant based on the diameter distribution model. *Forest Ecology and Management*, *260*(3), 339–344. https://doi.org/10.1016/j.foreco.2010.04.021

Yoro, K. O., & Daramola, M. O. (2020). CO2 emission sources, greenhouse gases, and the global warming effect. In *Advances in carbon capture* (pp. 3–28). Elsevier. https://doi.org/10.1016/B978-0-12-819657-1.00001-3

Yuan, W., Luo, Y., Liang, S., Yu, G., Niu, S., Stoy, P., Chen, J., Desai, A. R., Lindroth, A., Gough, C. M., Ceulemans, R., Arain, A., Bernhofer, C., Cook, B., Cook, D. R., Dragoni, D., Gielen, B., Janssens, I. A., Longdoz, B., . . . Varner, R. (2011). Thermal adaptation of net ecosystem exchange. *Biogeosciences*, *8*(6), 1453–1463. https://doi.org/10.5194/bg-8-1453-2011

Yuen, J. Q., Fung, T., & Ziegler, A. D. (2017). Carbon stocks in bamboo ecosystems worldwide: Estimates and uncertainties. *Forest Ecology and Management*, *393*, 113–138. https://doi.org/10.1016/j.foreco.2017.01.017

Zhou, G., Meng, C., Jiang, P., & Xu, Q. (2011). Review of carbon fixation in bamboo forests in china. *Bot. Rev.*, *77*(3), 262–270. https://doi.org/10.1007/s12229-011-9082-z

Appendices

A Resume table of allometric equation found in literature

ID	Bamboo species	Author (s) (year)	Location , region	Model	N (number of sampled bamboos)	R²	Error statistics
1	Bambusa balcooa	Nath , Das and Das (2009)	Barak Valley , India	log (AGB) = 2.476+ 0.997xlog (D)	NA	0.670	NA
2	Bambusa bambos	Shanmughavel and Francis (1996)	Kallipatty , India	log (AGB) = -0.3003 + 0.6804x log (D) + 1.0440xlog (H)	NA	0.990	NA
3	Bambusa bambos	Kumar , Rajesh and Sudheesh (2005)	Kerala	AGBclump = -3225.8 + 1730.4 x Dclump	8	0.830	NA
4	Bambusa bambos	Shanmughavel and Francis (1996 cited Yuen , Fung and Ziegler , 2017)	India	Bcu = 0.287 x D^3.524	NA	0.938	NA
5	Bambusa cacharensis	Nath , Das and Das (2009)	Barak Valley , India	log (AGB) = 2.114+ 1.087 x log (D)	NA	0.710	NA
6	Bambusa genus	Melo et al (2015)	Brazil	AGB = -0.5699 + 0.67696 x D^0.5 x log (D)	24	0.980	NA
7	Bambusa nutans	Yuen , Fung and Ziegler (2017)	Thailand	AGB = 0.269 x D^2.107	65	0.667	NA
8	Bambusa procera	Huy et al (2019b)	Vietnam	AGB = Bcu + Bbr + Ble = 0.09814 D^2.36569 +0.05216 D^2.00483+ 0.03044 D^1.74187	83	0.627 0.567 0.536 0.667	RMSE = 2.96, 0.77, 0.25, 3.58
9	Bambusa procera	Huy et al (2019b)	Vietnam	AGB = Bcu + Bbr + Ble = 0.02269 ((D^2)H)^0,90703 +0.02015 ((D^2)H)^0,72251 +0.03420 D^1.67330	83	0.631 0.488 0.535 0.649	RMSE = 2.95 , 0.84 , 0.25 , 3.62
10	Bambusa stenosstachya	L. Lin and Yen (2016)	Taiwan	AGB = 0.0262 x ((D^2)H)^0,9215	20	NA	RMSE = 3.9 MAPE = 11.5 %
11	Bambusa vulgaris	Nath , Das and Das (2009)	Barak Valley , India	log (AGB) = 1.404 + 2.073xlog (D)	NA	0.950	NA
12	Dendrocalamus barbatus	Ly et al (2012)	Vietnam	Bcu = 0.44 x (0.3002x D^2 + 0.115 xD)	131	0.920	NA
13	Dendrocalamus barbatus	Dung et al, (2012 cited Yuen , Fung and Ziegler , 2017)	Vietnam	Bcu = 0.113x D^2.102	100	0.883	NA
14	Guadua angustifolla	Ricardo et al (2013)	Bolovia	AGB = 2.6685 x D^0.9879	24	0.949	NA
15	Phyllostachys edulis (Moso bamboo)	Chen et al (2004 cited Kuehl , Lia and Henley , 2013)	China	AGB = -11.4970 + 3.0465 x D +0.1117 x D^2	NA	0.837	NA
16	Phyllostachys edulis	Nie (1994 cited Yuen , Fung and Ziegler , 2017)	China	Bcu = 0.0925xD^2.081	NA	0.998	NA
17	Phyllostachys edulis (Moso bamboo)	Zhou and Jiang (2004 cited Zhuang et al , 2015)	China	AGB = 747.787 x D^2.771 (0.148 x A / (0.028 + A))^5.555 +3.772	NA	NA	NA
18	Phyllostachys makinoi (Makino bamboo)	Yen , Ji and Lee (2010)	Taiwan	AGB = 0.156 x D^2.118	20	0.882	RMSE = 0.718
19	Phyllostachys makinoi (Makino bamboo)	Yen , Ji and Lee (2010)	Taiwan	AGB = 1.112 x D^2.695 x H^-1.175	20	0.898	RMSE = 0.688

Figure 26: Census of existing AGB models for bamboo species (derived from Huy and Long, 2019).

B Bamboo Atlas

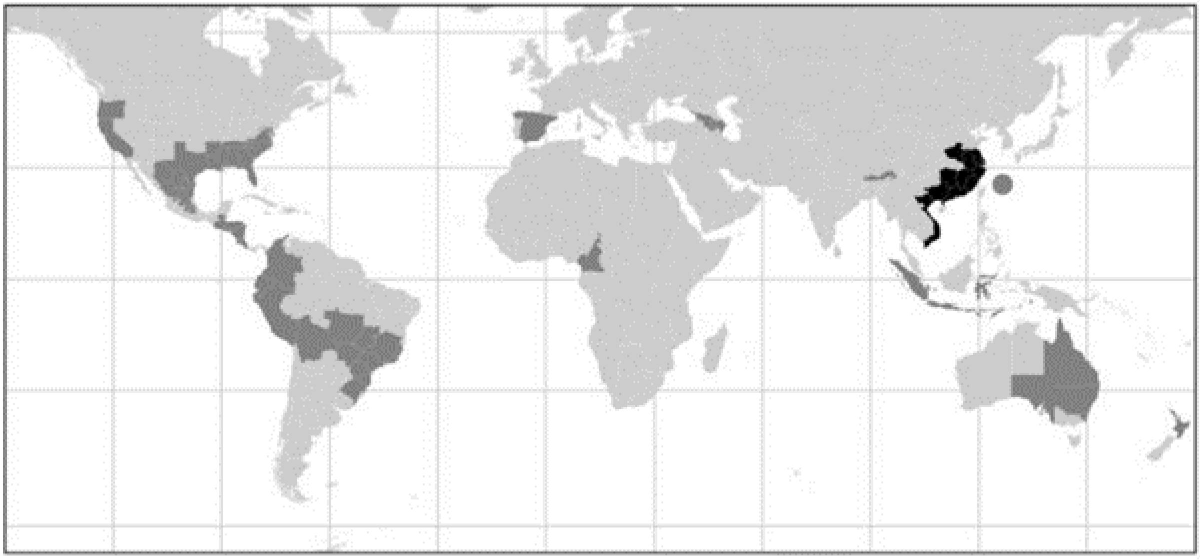

Figure 27: Known Areas where *Phyllostachys Aurea* grows natively (in black) and where it was introduced (in dark grey). Full name : *Phyllostachys aurea* (André) Rivière C.Rivière, Bull. Soc. Acclim. France, sér. 3, 5: 716 (1878).

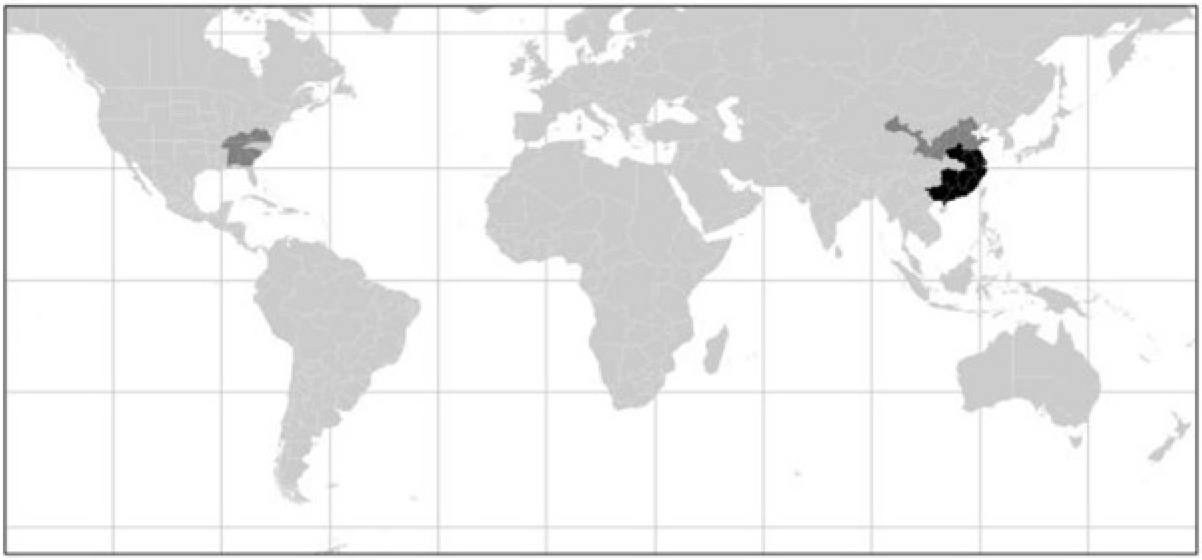

Figure 28: Known Areas where *Phyllostachys Aureosulcata* grows natively (in black) and where it was introduced (in dark grey). Full name : *Phyllostachys aureosulcata* McClure, J. Wash. Acad. Sci. 35: 282 (1945).

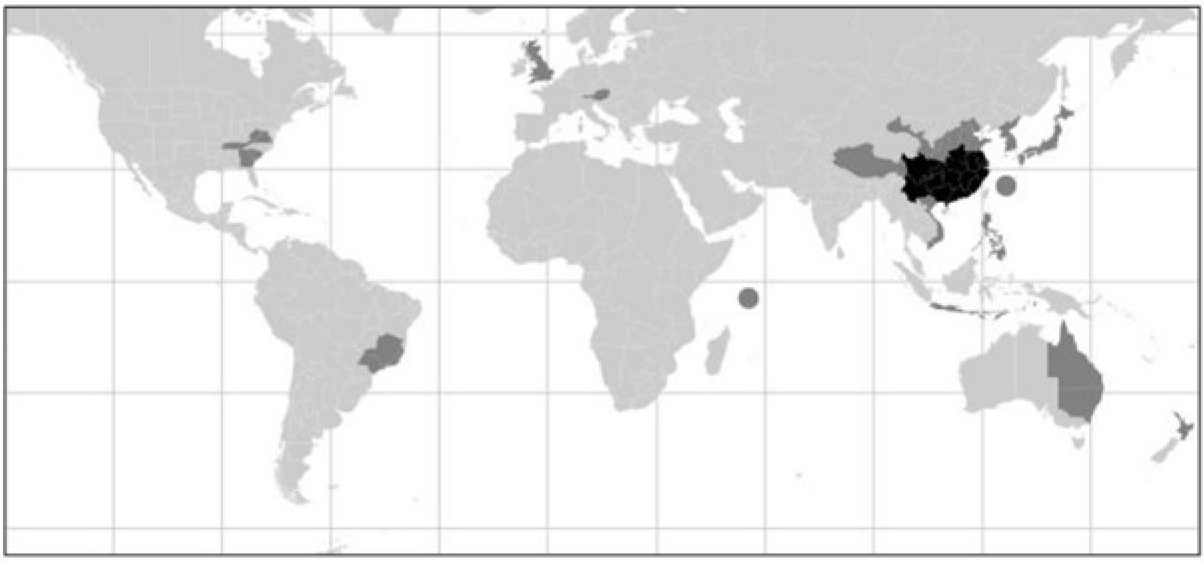

Figure 29: Known Areas where *Phyllostachys Nigra* grows natively (in black) and where it was introduced (in dark grey). Full name : *Phyllostachys nigra* (Lodd. ex Lindl.) Munro, Trans. Linn. Soc. London 26: 38 (1868).

C Tested Models

Data(N)	Model	Regression	weights	R2 (-)	R2adj (-)	AIC (-)	Bias (%)	RMSE (kg)	MAPE (%)
Mixed model (N=29 without J2 : measurements errors)									
29	log(AGB) = a + b × log (D)	lm	1/log(D)^2	-1.95	-2.31	88.27	-97.52	0.94	97.52
29	log(AGB) = a + b × log (H)	lm	1/log(H)^2	0.75	0.73	10.87	-8.18	0.27	29.16
29	AGB = a × D^b	nlme	varPower(form=~D)	0.92	0.91	-33.71	-5.62	0.16	19.97
29	AGB = a × H^b	nlme	varPower(form=~H)	0.88	0.87	-14.57	-7.51	0.19	27.65
29	log(AGB) = a + b × log (D) + c × log (H)	lm	1/(log(D) × log(H))^2	-261.15	-304.84	225.93	-1036.67	8.90	1036.67
29	log(AGB) = a + b × log (D) + c × log (H)	lm	1/(log(D))^2	-392.59	-458.19	236.65	-1242.98	10.91	1242.98
29	log(AGB) = a + b × log (D) + c × log (H)	lm	1/(log(H))^2	-575.09	-671.10	253.58	-1639.63	13.19	1639.63
29	AGB = a × D^b x H^c	nlme	varPower(form = ~D)						
29	AGB = a × D^b x H^c	nlme	varPower(form = ~H)	0.97	0.97	-48.40	-2.96	0.09	12.35
29	AGB = a × D^b x H^c	nlme	varPower(form = ~D+H)	0.97	0.97	-49.03	-2.79	0.09	12.42
29	AGB = a × D^b x H^c x ρ^d	nlme	varPower(form = ~D+H+ρ)	0.98	0.98	-56.14	-1.29	0.08	9.10
29	AGB = a × D^b x H^c x ρ^d	nlme	varPower(form = ~D)						
29	AGB = a × D^b x H^c x ρ^d	nlme	varPower(form = ~H)	0.98	0.98	-55.58	-1.43	0.08	9.10
29	AGB = a × D^b x H^c x ρ^d	nlme	varPower(form = ~ρ)						
29	AGB = a × D^b x H^c x ρ^d	nlme	varPower(form = ~D+H)	0.98	0.98	-56.15	-1.43	0.08	9.04
29	AGB = a × D^b x H^c x ρ^d	nlme	varPower(form = ~D+ρ)						
29	AGB = a × D^b x H^c x ρ^d	nlme	varPower(form = ~H+ρ)	0.9801117	0.9757882	-55.7610400	1.2347890	0.0775244	9.18
29	log(AGB) = a + b × log (D) + c x log (H) + d x log(ρ)	lm	1/(log(D) x log(H) x log(ρ))^2	-1392.25	-1624.46	287.89	-2699.88	20.52	2699.88

Figure 30: List of the Multi species models tests.

Phyllostachys Aurea N=10									
Data(N)	Model	Regression	weights	R2	R2adj	AIC	Bias	RMSE	MAPE
10	log(AGB) = a + b × log (D)	lm	1/log(D)^2	0.7505478	0.6258218	-0.6279406	-52.23162	0.1841996	55.41846
10	log(AGB) = a + b × log (H)	lm	1/log(H)^2	0.9818767	0.972815	-27.6238	-0.5107438	0.0496494	7.158679
10	AGB = a × D^b	nlme	varPower(form=~D)	0.8625668	0.7938503	-4.84288	-7.796187	0.1367227	23.73113
10	AGB = a × H^b	nlme	varPower(form=~H)	0.9813997	0.9720995	-27.49543	-0.6784312	0.05029854	7.158179
10	log(AGB) = a + b × log (D) + c × log (H)	lm	1/(log(D) x log(H))^2	-1129401	-2032923	159.56	-62350.39	391.9397	62350.39
10	log(AGB) = a + b × log (D) + c × log (H)	lm	1/(log(D))^2	-1034191	-1861545	158.6404	-59450.27	375.0556	59450.27
10	log(AGB) = a + b × log (D) + c × log (H)	lm	1/(log(H))^2	-710685.1	-1279234	154.5833	-48246.75	310.9094	48246.75
10	AGB = a × D^b x H^c	nlme	varPower(form = ~D)						
10	AGB = a × D^b x H^c	nlme	varPower(form = ~H)	0.9504036	0.9107264	-24.97365	0.2688226	0.08213347	7.042067
10	AGB = a × D^b x H^c	nlme	varPower(form = ~D+H)	0.955543	0.9199774	-23.87916	0.4533879	0.07776158	6.990813
10	AGB = a × D^b x H^c x ρ^d	nlme	varPower(form = ~D+H+ρ)						
10	AGB = a × D^b x H^c x ρ^d	nlme	varPower(form = ~D)						
10	AGB = a × D^b x H^c x ρ^d	nlme	varPower(form = ~H)	0.9485925	0.8843331	-14.98585	0.2940712	0.08361965	7.13183
10	AGB = a × D^b x H^c x ρ^d	nlme	varPower(form = ~ρ)	0.9522715	0.8926109	-20.53538	-0.7988865	0.08057193	6.738842
10	AGB = a × D^b x H^c x ρ^d	nlme	varPower(form = ~D+H)						
10	AGB = a × D^b x H^c x ρ^d	nlme	varPower(form = ~D+ρ)						
10	AGB = a × D^b x H^c x ρ^d	nlme	varPower(form = ~H+ρ)	0.9528844	0.8939899	-14.68797	-0.2734807	0.08005295	6.759451
10	log(AGB) = a + b × log (D) + c x log (H) + d x log(ρ)	lm	1/(log(D) x log(H) x log(ρ))^2	-524539	-944171	153.8419	-42810.72	267.1064	42810.72

Figure 31: List of the *P.Aurea* models tests.

Data(N)	Model	Regression	weights	R2 (-)	R2adj (-)	AIC (-)	Bias (%)	RMSE (kg)	MAPE (%)
Mixed model (N=29 without J2 : measurements errors)									
29	log(AGB) = a + b × log (D)	lm	1/log(D)^2	-1.95	-2.31	88.27	-97.52	0.94	97.52
29	log(AGB) = a + b × log (H)	lm	1/log(H)^2	0.75	0.73	10.87	-8.18	0.27	29.16
29	AGB = a × D^b	nlme	varPower(form=~D)	0.92	0.91	-33.71	-5.62	0.16	19.97
29	AGB = a × H^b	nlme	varPower(form=~H)	0.88	0.87	-14.57	-7.51	0.19	27.65
29	log(AGB) = a + b × log (D) + c × log (H)	lm	1/(log(D) × log(H))^2	-261.15	-304.84	225.93	-1036.67	8.90	1036.67
29	log(AGB) = a + b × log (D) + c × log (H)	lm	1/(log(D))^2	-392.59	-458.19	236.65	-1242.98	10.91	1242.98
29	log(AGB) = a + b × log (D) + c × log (H)	lm	1/(log(H))^2	-575.09	-671.10	253.58	-1639.63	13.19	1639.63
29	AGB = a × D^b x H^c	nlme	varPower(form = ~D)						
29	AGB = a × D^b x H^c	nlme	varPower(form = ~H)	0.97	0.97	-48.40	-2.96	0.09	12.35
29	AGB = a × D^b x H^c	nlme	varPower(form = ~D+H)	0.97	0.97	-49.03	-2.79	0.09	12.42
29	AGB = a × D^b x H^c x ρ^d	nlme	varPower(form = ~D+H+ρ)	0.98	0.98	-56.14	-1.29	0.08	9.10
29	AGB = a × D^b x H^c x ρ^d	nlme	varPower(form = ~D)						
29	AGB = a × D^b x H^c x ρ^d	nlme	varPower(form = ~H)	0.98	0.98	-55.58	-1.43	0.08	9.10
29	AGB = a × D^b x H^c x ρ^d	nlme	varPower(form = ~ρ)						
29	AGB = a × D^b x H^c x ρ^d	nlme	varPower(form = ~D+H)	0.98	0.98	-56.15	-1.43	0.08	9.04
29	AGB = a × D^b x H^c x ρ^d	nlme	varPower(form = ~D+ρ)						
29	AGB = a × D^b x H^c x ρ^d	nlme	varPower(form = ~H+ρ)	0.9801117	0.9757882	-55.7610400	1.2347890	0.0775244	9.18
29	log(AGB) = a + b × log (D) + c x log (H) + d x log(ρ)	lm	1/(log(D) x log(H) x log(ρ))^2	-1392.25	-1624.46	287.89	-2699.88	20.52	2699.88

Figure 32: List of the *P.Aureosulcata* models tests.

Data(N)	Model	Regression	weights	R2 (-)	R2adj (-)	AIC (-)	Bias (%)	RMSE (kg)	MAPE (%)
Mixed model (N=29 without J2 : measurements errors)									
29	log(AGB) = a + b × log (D)	lm	1/log(D)^2	-1.95	-2.31	88.27	-97.52	0.94	97.52
29	log(AGB) = a + b × log (H)	lm	1/log(H)^2	0.75	0.73	10.87	-8.18	0.27	29.16
29	AGB = a × D^b	nlme	varPower(form=~D)	0.92	0.91	-33.71	-5.62	0.16	19.97
29	AGB = a × H^b	nlme	varPower(form=~H)	0.88	0.87	-14.57	-7.51	0.19	27.65
29	log(AGB) = a + b × log (D) + c × log (H)	lm	1/(log(D) × log(H))^2	-261.15	-304.84	225.93	-1036.67	8.90	1036.67
29	log(AGB) = a + b × log (D) + c × log (H)	lm	1/(log(D))^2	-392.59	-458.19	236.65	-1242.98	10.91	1242.98
29	log(AGB) = a + b × log (D) + c × log (H)	lm	1/(log(H))^2	-575.09	-671.10	253.58	-1639.63	13.19	1639.63
29	AGB = a × D^b x H^c	nlme	varPower(form = ~D)						
29	AGB = a × D^b x H^c	nlme	varPower(form = ~H)	0.97	0.97	-48.40	-2.96	0.09	12.35
29	AGB = a × D^b x H^c	nlme	varPower(form = ~D+H)	0.97	0.97	-49.03	-2.79	0.09	12.42
29	AGB = a × D^b x H^c x ρ^d	nlme	varPower(form = ~D+H+ρ)	0.98	0.98	-56.14	-1.29	0.08	9.10
29	AGB = a × D^b x H^c x ρ^d	nlme	varPower(form = ~D)						
29	AGB = a × D^b x H^c x ρ^d	nlme	varPower(form = ~H)	0.98	0.98	-55.58	-1.43	0.08	9.10
29	AGB = a × D^b x H^c x ρ^d	nlme	varPower(form = ~ρ)						
29	AGB = a × D^b x H^c x ρ^d	nlme	varPower(form = ~D+H)	0.98	0.98	-56.15	-1.43	0.08	9.04
29	AGB = a × D^b x H^c x ρ^d	nlme	varPower(form = ~D+ρ)						
29	AGB = a × D^b x H^c x ρ^d	nlme	varPower(form = ~H+ρ)	0.9801117	0.9757882	-55.7610400	1.2347890	0.0775244	9.18
29	log(AGB) = a + b × log (D) + c × log (H) + d x log(ρ)	lm	1/(log(D) x log(H) x log(ρ))^2	-1392.25	-1624.46	287.89	-2699.88	20.52	2699.88

Figure 33: List of the *P.Nigra* models tests.

D Leaf nets data

leaf nets			
date	plot	weight (g)	
17-mai	Noir	perforated net	
	vert	7.81	
	Jaune	3.86	(1)
	jaune	7.22	(2)
	jaune	5.9	(3)
08-juil	Noir	27.4	
	Vert	broken leaf net	
	jaune	54.06	(1)
	jaune	34.45	(2)
	jaune	36.14	(3)

Figure 34: Weight of leaves harvested with the nets.

E Moisture Content (%)

MC_IN	MC_N	MC_M
56.76	43.75	50.26
0.00	0.00	0.00
37.96	37.47	37.72
47.16	33.18	40.17
35.05	35.24	35.15
56.27	34.44	45.35
56.12	39.01	47.57
58.27	34.24	46.26
33.71	25.13	29.42
57.27	36.83	47.05
64.63	47.50	56.07
71.54	52.08	61.81
67.84	53.92	60.88
50.51	52.54	51.53
46.99	43.91	45.45
64.89	43.63	54.26
39.10	28.94	34.02
56.74	36.59	46.66
39.92	26.40	33.16
56.78	47.17	51.98
41.67	38.16	39.91
35.77	34.64	35.20
56.60	29.41	43.01
47.50	46.34	46.92
49.52	50.20	49.86
45.82	44.12	44.97
35.81	39.63	37.72
50.07	32.33	41.20
77.87	45.81	61.84
27.78	19.87	23.82

Figure 35: Moisture content in % for Internodes (MCIN) Nodes (MCN) and the mean of both (MCM).